Bachelor's Thesis
Faculty of Science and Technology

Designing a Laser Scanning Confocal Microscope: A new scan engine layout

David van Duinen

Bachelor assignment committee:
Chairman - Dr. ir. Herman Offerhaus
Daily supervisor - Erik Garbacik Msc.
External member - Dr. Ir. Mark Huijben
Member - Ing. Jeroen Korterik

July 1st 2013

UNIVERSITY OF TWENTE.

ABSTRACT

Background

For several optical imaging systems a scan engine is used. The currently used scan engines use 2 mirrors and, although this makes the scanning fairly easy it also introduces a inherent error in the beam's position. The targeted application for the newly designed scan engine is a laser scanning confocal microscope.

Approach

The error introduced originates from the mirrors having different deflection origins. To displace one of the origins to coincide a third, correcting mirror can be introduced. However, when another, fourth mirror is introduced both origins can be controlled in space and hence a full 3D control of this point is obtained.

Also the scan mirrors and their controls and feedback systems have been characterized. The system used is a "High speed Galvo System, AXJ-V20 close-loop scanner". Yet before this the system was optimized as some settings were adjustable.

Results

An expression for a pivot point was analytically found, as function of the angles of all four scan mirrors. The system seemed too coupled to solve analytically and hence a numerical approach using a covariant matrix adaptation evolution strategy was tried. This resulted in a set of angles for which the pivot point remained stationary.

The system was optimized and its response for several frequencies and deflections were obtained.

Conclusions

The newly designed scan system can be applied in a microscope or imaging system. The galvanometers have been characterized and thus is ready for operation.

CONTENTS

CHAPTER 1

INTRODUCTION

Imaging has been around for ages. Since the evolution of the first light detecting cells organisms have been able to notice the world through vision. As time progressed the eye evolved, using lenses to be able to focus at various depths. The ancient Greeks studied the interaction that light had with matter and millennia later the first lenses were produced, introducing a very important component for modern day optical instruments. Later in the 16^{th} and 17^{th} centuries the first microscopes were designed by great names in physics like Galileo Galilei and Christiaan Huygens. These microscopes changed the way people saw the world. Even now microscopes change our view on the world. Although, the differences between the 17^{th} century's microscope and the Large Hadron Collider at CERN are enormous their aims are similar: to view this world on a different level than usual.

One type of microscope is the laser scanning confocal microscope (LSCM), invented by Marvin Minsky in 1957 [5]. This type of microscope nowadays has most of its applications in biology as it able to produce very crisp images, also *in vivo*. Figure 1.1b shows an image produced by the LSCM's principle.

1.1 The LSCM

A LSCM can be broken down into two parts: laser scanning and the confocal microscopy. The confocal microscope is unique amongst other types of microscopes as it gives the user control over the imaging depth. Moreover it produces a clearer image; an enhanced resolution because of the confocal pinhole, filtering out the non-focal light [1]. While laser scanning is not the principle technique the LSCM, it provides a reasonably big advantage as the sample itself can now remain stationary.

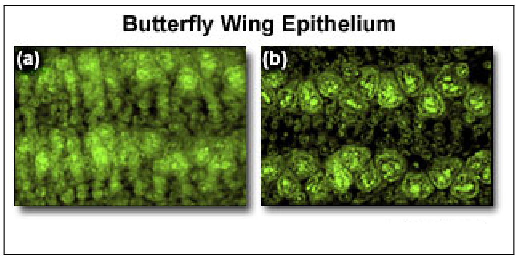

Figure 1.1: Comparison of conventional wide field microscope [left] to confocal microscopy [right]. Source: http://www.microscopyu.com/ [1].

1.2 The confocal microscope optical train

The optical train and its working principle[1] has been depicted in figure 1.2. It consists of no more than a pinhole and some ray directing components. The light originates from a laser from the left. This light will be used to interact with the sample, e.g. to induce fluorescence or simple absorption. In order to get as much interaction with the sample this light is focussed through an objective lens. As it is not possible to prevent unfocussed light to interact with the sample as well, more than one point source will appear in

[1] This only shows the principle of <u>confocal</u> microscopy; it is therefore, no LSCM.

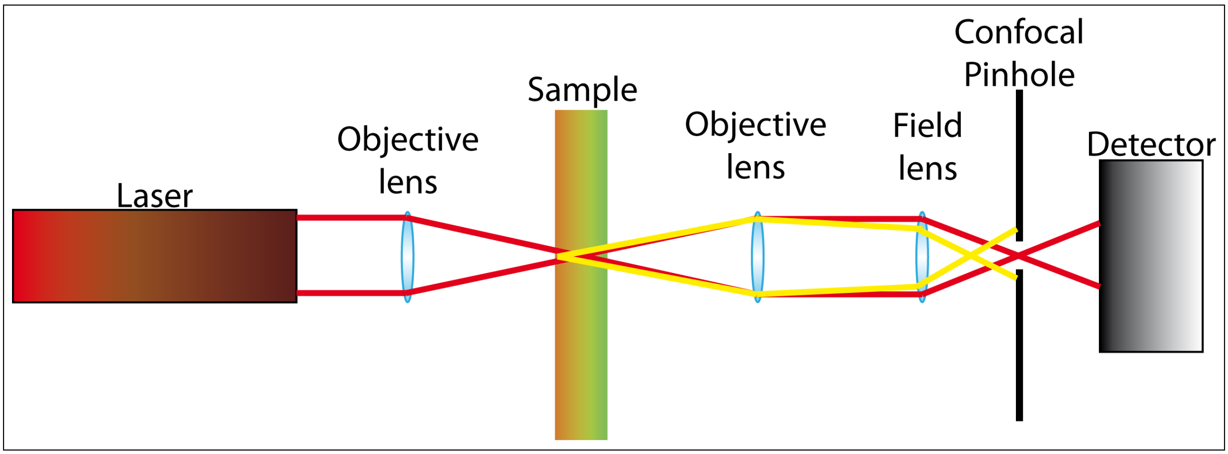

Figure 1.2: Principle light pathways in confocal microscopy, transmission mode. This is not a full LSCM, only a confocal microscope's principles.

the sample (depicted by a red and yellow beam in the figure). The sample's light will then be collected by a set of lenses. The first lens has been calibrated to have its focus confocally with the objective lens. The red rays are originating from the focus of the objective lens and hence a collimated beam will result. When this collimated beam is again focussed by a lens it can be directed through a pinhole, after which the light is detected by a detector.

The yellow rays, however, do not originate from the foci. Therefore, this light will not be collimated. Thus resulting in another focus of the last lens. As the pinhole is set on the focus of a collimated beam the yellow rays will not have a focus inside the pinhole and hence will be filtered out [1].

This example shows a transmission mode imaging confocal microscope. Since fluorescence is possible also reflection mode imaging is used. In reflection mode the laser beam and the sample beam share part of the optical path a dichroic mirror is often used, reflecting only the laser light and allowing other wavelengths.

A result is shown in figure 1.1, in which a comparison is made between a conventional wide field microscope and a confocal microscope. The imaged sample is a butterfly pupal wing epithelium stained with propidium iodide. The right image has a higher resolution than the wide field image due to the spatial filtering. The nuclei of the cells are now clearly visible.

1.3 Laser scanning

The laser scanning of the LSCM is achieved through a scan engine. The scan engine of of a LSCM can exist of a variety of different controllable mirrors. The only demand for the scan engine is that it can scan a 2D sample within certain requirements: e.g. sampling speed and resolution. Most microscopes use two 1D galvanometers or a combination of a galvanometer and a rotating polygonal prism mirror [8].
In figure 1.3 the output of a scan engine (in 1D) is drawn as either one colour of the lines at different angles: blue, red or green. As the output angle of the scan engine varies this gets translated into a displacement on the sample, after the objective, due to the scan- and tube-lens[2]. In most lens systems a magnification is also incorporated by having two lenses of different focal length.

The Optical Sciences group (OS) at the University of Twente uses a type of LSCM in some of their experiments [2]. This LSCM uses a scan engine existing of two mirrors. This is easiest to operate but

[2]A simple applet showing this principle can be found at: http://www.olympusfluoview.com/java/aperturescanner/index.html.

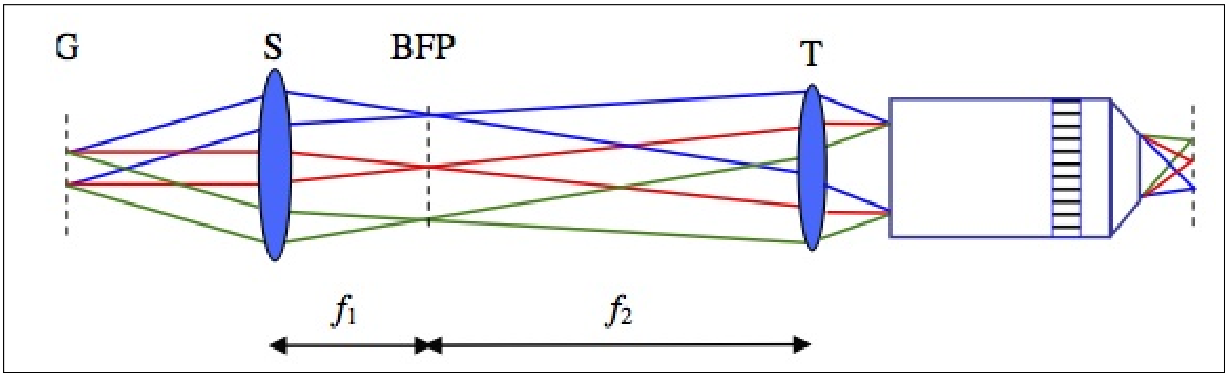

.

Figure 1.3: The configuration of the scanning system of a LSCM. G: Galvanometer; S: scan-lens; BFP: back focal plane; T: tube-lens; f1: focal length of S; f2: focal length of T [8].

it comes with a price. As seen in figure 1.3, one function of the lenses is to focus the laser onto the objective. However, in the 2D system, using two mirrors, this is not possible as the mirrors cannot both be placed in the focus of the lens. Therefore, the focus produced on the objective is not a perfect 2D focus.

This is what we attempted to improve in the current LSCMs. The design for a new scan engine includes another two mirrors, thereby resulting in a true stationary point. One other other advantage of using a total of 4 mirrors is that it gives full 3D control of where to put the stationary point. Therefore, small adjustments may be achieved by the system itself by simply programming the mirrors.

Other chapters

Chapter 2 gives several mathematical descriptions of the scan engine. The characterization and measurements of the mirrors will be discussed in chapter 3, after which a combination of these findings and theory will be discussed shortly. The report will then be concluded and some recommendations will be given in chapters 4 and 5 respectively.

CHAPTER 2

SCAN ENGINE

2.1 Introduction

If a laser scanning confocal microscope is to work optimally, it is important that the beam originates from a stationary point, exactly in the focus of the rest of the optics. When the condition is met that this point is stationary in time it functions; able to assume various angles so scanning is possible. In order to achieve a stationary point a new system using 4 mirrors was developed, shown in figure 2.1.

The current LSCMs use two mirrors in the scan engine. The problem this brings about is that both mirrors do not share the same pivoting point. Hence the total system can never be perfectly aligned and aberrations will always be a part of the setup. However, introducing a third compensation mirror will remove this flaw. Introducing another mirror: a second mirror for each scan plane will give full spatial control over the pivot point. Each of these mirrors has its own galvanometer (GM) and hence can be easily operated, independently from the other GMs.

Designing this system involves two main fields. One is creating a theoretical model so the scan engine can be operated and an actual stationary point can be produced. The other field is to characterise the GMs, as the signal transfer is unknown.

2.2 General layout of the scan engine: XYXY

The scan engine can be segmented into 5 parts, as seen in figure 2.1:

A: Laser - first mirror (X1)

B: X1 mirror - Y1 mirror

C: Y1 mirror - X2 mirror

D: X2 mirror - Y2 mirror

E: (Y2 mirror - stationary point)

Note that the stationary point can also be on or even before the last mirror (Y2), as this would still work as a focus for the lens.

In order to not overcomplicate the model a several aspects have been left out such as the dimensions of the mirrors and their maximum deflections. To keep the model valid more boundary conditions should be set. This should be done by looking at the obtained deflections of the mirrors. From these reflections it is relatively easy to find the locations where the beam will hit the mirror, for which the boundary conditions were applied; this can be done after the calculations as an extra check.

To identify the angles to use for a stationary point first of all the scan engine had to be described well. From this mathematical description it would then be possible to lay some boundary conditions to it:

$$\frac{\partial\,(\text{expression for the stationary point})}{\partial\,(\text{any GM angle})} = 0 \tag{2.1}$$

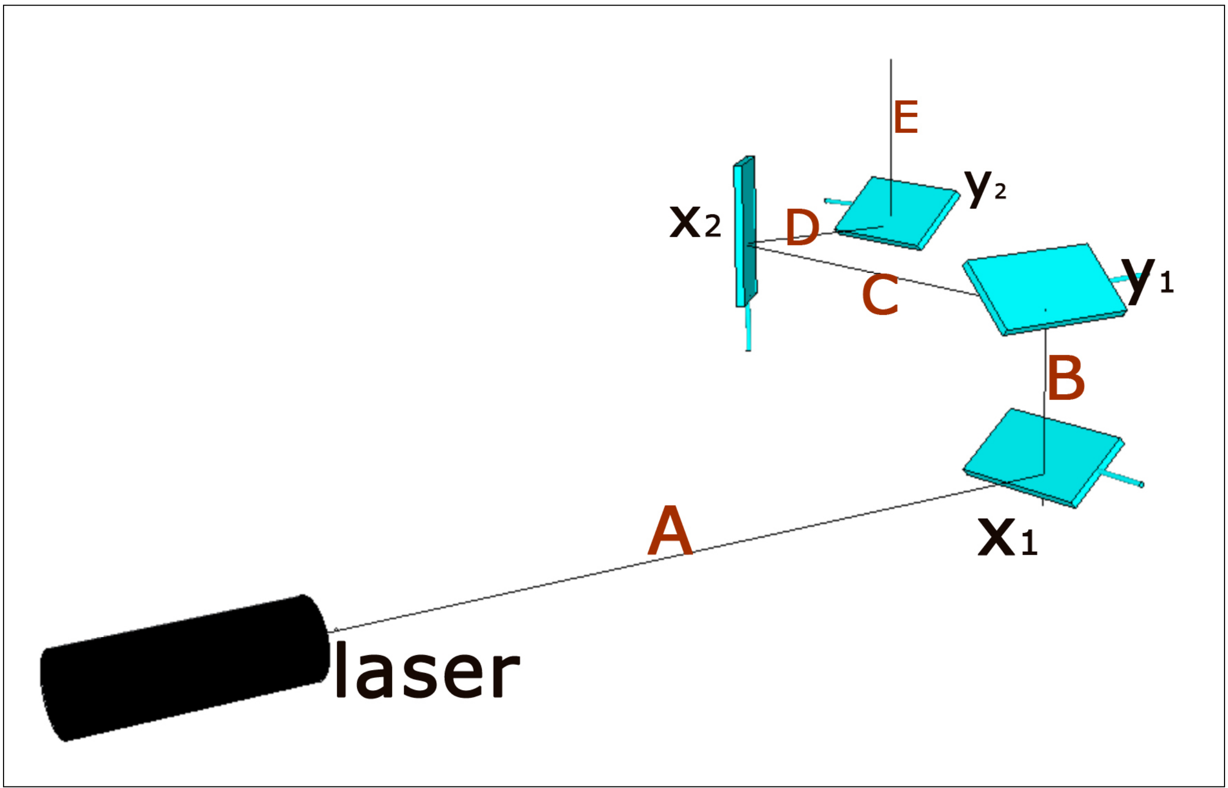

Figure 2.1: Lay out of the scan engine and its mirrors: X1, Y1, X2 and Y2. In this setting the scan area would be in the z, x plane but this can easily be changed by adding another 45°mirror to convert it to the x, y plane. For the rest of the equations in the report a XY-scan area has been used, hence the mirrors are X1, X2 and Y1, Y2.

As long as this condition is met the stationary point will in fact be stationary: the derivatives of the position with respect to the angles equals 0. The ultimate goal is to find a relation between the GM angles from equation 2.1.

2.3 General Derivations

Deriving the expression for the stationary point

To determine each ray segment figures 2.2 and 2.3 were used. Since not all ray segments propagate in the same direction a different set of coordinates was used so it would be applicable for every ray segment.

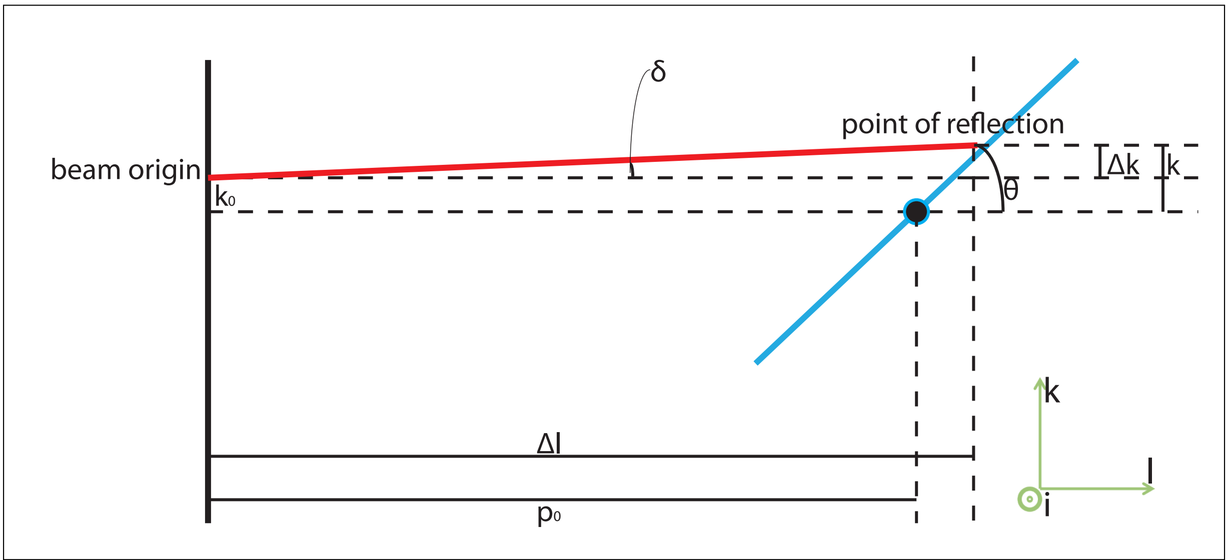

Figure 2.2: The Cheatsheet, I and k view.

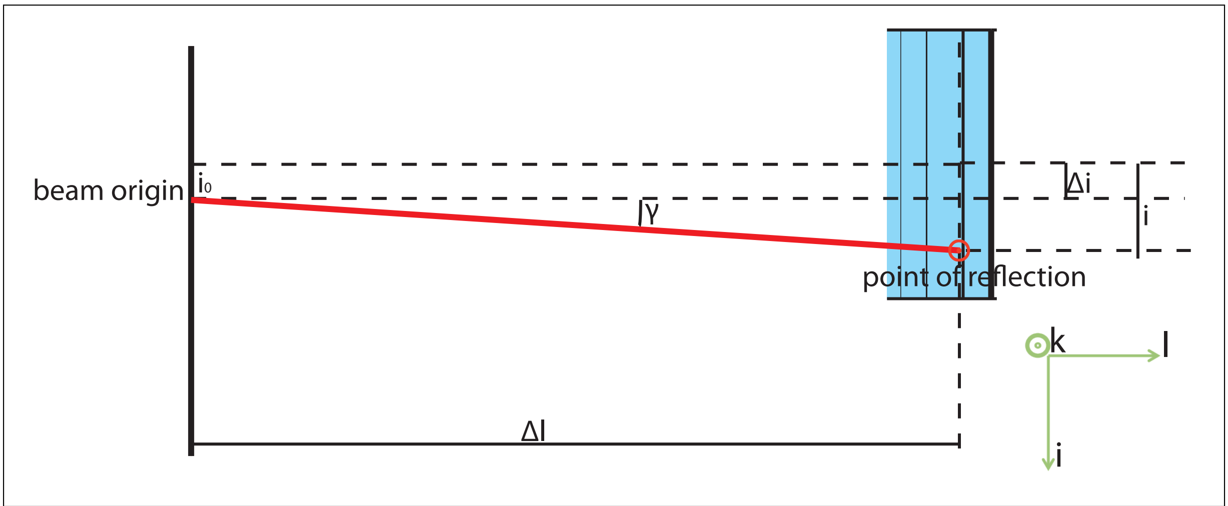

Figure 2.3: The Cheatsheet, I and i view.

In these figures the beam originates from the left side and hits a mirror at the right. Figure 2.2 and figure 2.3 give different points of view of the same situation. As the beam will not always hit one mirror axially there is an offset in all variables at the origin of the ray: angles δ and γ and on the I, k and i coordinates: l_0, k_0 and i_0. Using the figures it is then possible to derive changes in the coordinates, $\Delta l, \Delta k$ and Δi. After the rays have reflected upon the mirrors they will have gained an additional angle θ[1].

Now $\Delta l, \Delta k$ and Δi can be determined[2]:

$$\Delta l = \frac{p_0 \tan(\theta) - k_0}{\tan(\delta) - \tan(\theta)} \tag{2.2}$$

$$\Delta k = \frac{p_0 \tan(\theta)\tan(\delta) - k_0 \tan(\delta)}{\tan(\delta) - \tan(\theta)} \tag{2.3}$$

$$\Delta i = \frac{p_0 \tan(\theta)\tan(\gamma) - k_0 \tan(\gamma)}{\tan(\delta) - \tan(\theta)} \tag{2.4}$$

In equations 2.2, 2.3 and 2.4 all variables represent a different value in segments A-E. The results of the calculations for the pivot point, $\vec{PP}$, can be found in appendix A. For $\vec{PP}$ an extended equation was found[3,4]. With exception of the y component, as this only indicates the distance from the last mirror to $\vec{PP}$. The expressions for $\vec{PP}_x$ or $\vec{PP}_z$ also seem coupled as both are functions of all four angles: $\theta_1, \theta_2, \phi_1$ and ϕ_2. Angles θ_1 and θ_2 belong to mirrors X1 and X2, respectively and ϕ_1, ϕ_2 to Y1 and Y2, respectively.

2.4 Boundary conditions

The partial derivative with respect to any angle should equal 0 (equation 2.1) this results in:

$$\frac{\partial PP}{\partial \theta_1} = \frac{\partial PP}{\partial \theta_2} = \frac{\partial PP}{\partial \phi_1} = \frac{\partial PP}{\partial \phi_2} = 0 \tag{2.5}$$

2.5 Analytical approach
Trial and error

Several methods have been tried to find a relation for the angles. These methods are shown in the following paragraphs.

2.5.1 Partial derivatives

As equation 2.5 shows there are in total 4 equations that lead to the solution. These derivatives have been done by using Maple. The four partial derivatives gave only larger expressions than $\vec{PP}$. When trying to solve the partial derivatives equalled to zero maple did not find a sensible expression. The results produced by Maple still included $RootOf$ and $\_Z$ expressions, still were dependent on all other angles and often extended beyond one page in size, therefore not giving a feasible solution.

[1] θ has been used as a arbitrary variable. It is not the same as the angle belonging to the x-mirror.
[2] For the full derivation, see Appendix A.
[3] In deriving the beam's positions Maplesoft's Maple 17.00 was used.
[4] Note also that $\vec{PP}$ is a vector. When in some equation "PP" is written, only one of the variables x, y or z is meant

2.5.2 Taylor series

To try another approach and perhaps simplify the expressions, the first order Taylor expansions were taken and equaled to zero. The Taylor series with respect to θ_1 and ϕ_1 were taken as these are the correction mirrors, which will deflect only slightly, therefore validating the use of the Taylor expansion. There are a total of 8 useful equations: equation 2.5 for PP_x and PP_z. Doing Taylor expansions on all of them for θ_1 and ϕ_1 will double this to 16 equations, equated to 0. Yet, this proved not to be sufficient and no useful equations were found, because of similar reasons as stated at section 2.5.1. The best equation obtained used the first order Taylor expansion of PP_z with respect to ϕ_1. Solving this for θ_2 resulted in a 2-term expression, but still as a function of θ_1 and ϕ_2.

As this did not work out also the Taylor expansions with respect to θ_2 and ϕ_2 were taken. This resulted in similar expressions as for previously mentioned Taylor expansion solutions.

2.5.3 Small angle approach

In the expression for $\vec{PP}$ many $\tan(...)$ type functions with small arguments occur. Therefore, a small angle approach could be made where $\tan(\theta) = \theta$, where θ is either θ_1 or ϕ_1.

As this did not give sensible expressions it was expanded to also include the terms like: $\tan(\pm\frac{\pi}{4} + \theta)$ (where θ can equal θ_1 or ϕ_1). However, this also did not yield any useful relations for the angles.

2.5.4 Linear relation

Intuitively we expected that θ_1 and θ_2 (or ϕ_1, ϕ_2) would have some linear relation, depending on the distances between the mirrors. Therefore an approach was attempted where θ_1 and ϕ_1 would be substituted by $k\theta_2$ and $m\phi_2$ respectively. Then only the derivatives with respect to θ_2 and ϕ_2 would have to be done, while there would still be 4 equations ($PP_{x,\theta_2} = PP_{x,\phi_2} = PP_{z,\theta_2} = PP_{z,\phi_2} = 0$) and 4 variables ($\theta_2$, ϕ_2 and k and m); therefore theoretically solvable.
This also did not provide a feasible expression for solving the situation.

2.5.5 A different mirror layout

The analytical approach for obtaining a stationary $\vec{PP}$ did not succeed as the expression for x (or z) is dependent on more than two angles. Therefore, another configuration was investigated which intuitively seems less coupled. A YXXY setup was tried, as seen in figure 2.4. The general derivation (using i, k and l) would still be valid in this setup as the beams still originate from some point and hit a mirror under an angle. When the beam's coordinates would again be derived with help of the Cheatsheet coupling would still occur.

Even though there is still not a useful expression for the angles this exercise has not been done in vain. This setup shows a lot clearer where the coupling comes from; in figure 2.5 this is made visible. When just the effect of the x mirrors is investigated, it seems like a very uncoupled system and this is indeed the case until mirror X2. The final x deviation is $w\tan(\alpha)$. However, at the right hand of the figure it is seen that the path lengths of the red and yellow lines differ, depending on the optical path due to the Y mirrors: the distance w is a function of the deflections of the y-mirrors. This is also the case when calculating y-deflection, the distance between the mirrors will vary due to the deflections of the x-mirrors.

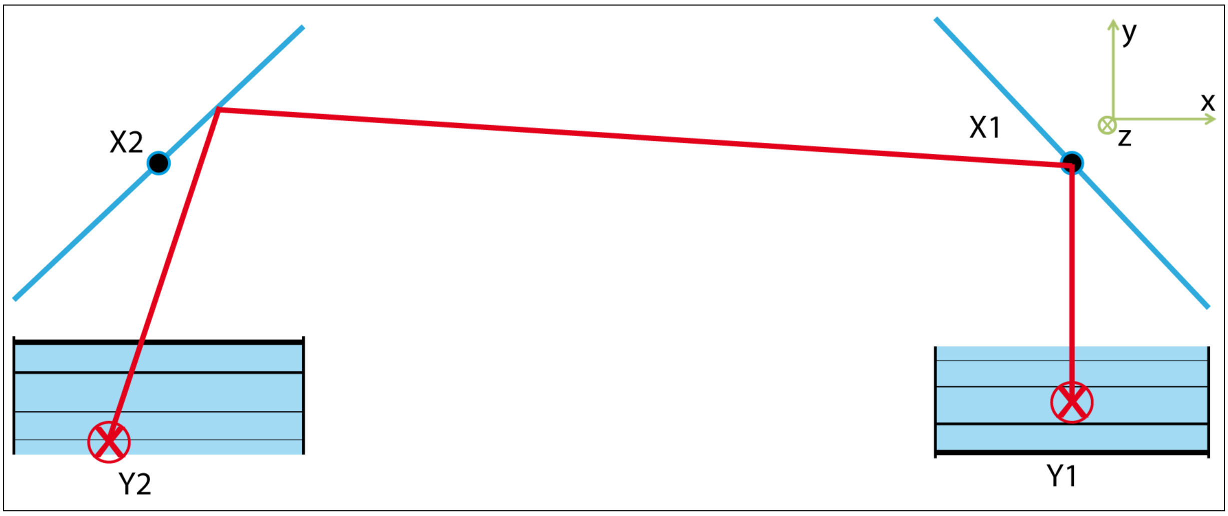

Figure 2.4: Other layout for the scan engine: YXXY, the beam going from right to left. Note that the reflections upon the mirrors are not physical, the focus should be put on the beams as these account for the path lengths and hence coupling of Y mirrors in the x plane and vice versa.

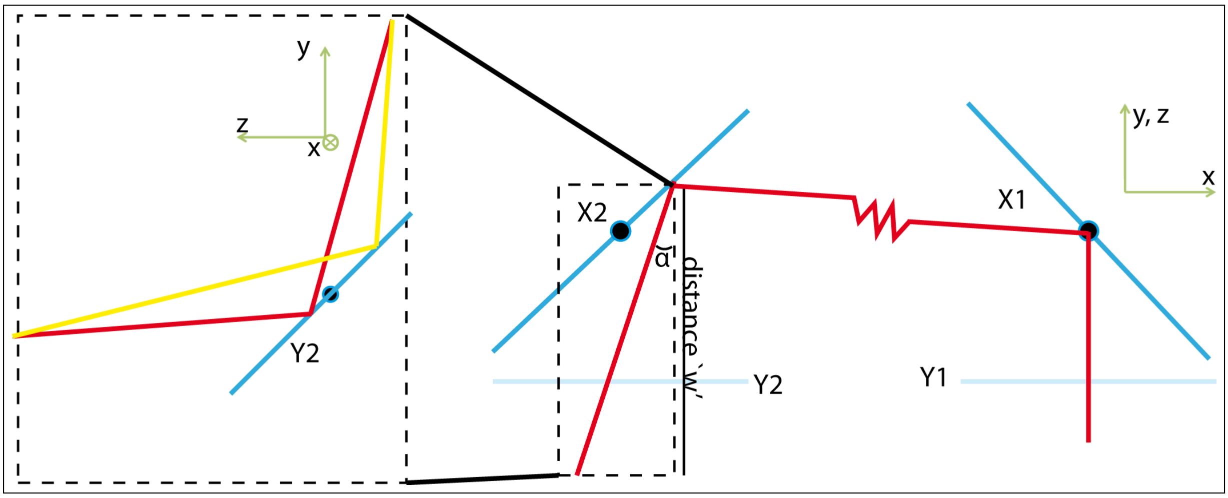

Figure 2.5: YXXY configuration with extra view of last beam part (X2 - PP).

2.5.6 Analytical approach: conclusion

The scan engine system seems comprehendible but after several simplifications no useful expression was found: the system's x and y were coupled. At first an attempt was made whereby no simplifications were implemented. Simplifying by assuming the angles are small: taking the first order Taylor expressions were tried, as well as substituting several functions with easier functions. Also linear relations between θ_1 and θ_2 and ϕ_1 and ϕ_2 were tried but did not provide a useful solution.

Lastly a different layout was studied. Although, it did not provide a useful solution it did give further insight in the scan engine system.

2.6 Numerical approach

The analytical approach did not provide a relation for any of the angles to provide a stationary point. However, it did give an expression for the beam's position. This expression is still useable for a numerical, brute-force approach: calculate for many deflections and pick out the right, useful results.

2.6.1 Evolutionary algorithm

To find approximations to the best possible fits for the position and angle of the beam (at PP), an evolutionary algorithm was used. The CMA, Covariance Matrix Adaptation [3] algorithm was used. Going into the details of this algorithm is beyond the scope of this thesis and hence only the theoretical surface will be explained[5].

The basic algorithm looks like this:

```
addpath c:\CMA_or_whatever_else_the_foldername_is
genes = Initialization('myoptions.m');

for i=1:NumberOfGenerations
  %% Do something with these genes; measure a fitness for every individual
  genes = NextGeneration(fitness);
end
```

A single for loop where only genes are changed and a fitness is produced, which gets saved and expanded in a "genes" array.

The algorithm consists of a number of generations, each with a number of individuals and each individual has its own number of genes. In a nutshell the algorithm thus acts like Darwin's evolution theorem with a predefined fitness[6]. The algorithm then makes a selection of the individuals based on their fitness, e.g. the fitness should be as high as possible, therefore the 5 individuals with highest fitness number 'survive' onto the next generation. For the next generation a total number of 10 individuals is required so 5 more are created. These are based on the surviving individuals, therefore converging to the best fitting case.

In the case of the scan engine the genes were the 4 deflection angles: θ_1, θ_2, ϕ_1 and ϕ_2. An individual is the position of the beam and the related angles: $\vec{PP}$, α_e and β_e.
To determine a fitness some ideal, demanded, values for $\vec{PP}$, α_e and β_e need to be set. For the fitness the differences of individual and demand are then weighed using a weighing factor W. W normalizes the value it belongs to, therefore it becomes possible to use both the position and the angles. The magnitude of W has been determined to be the approximated[7] maximum values: for the positions it is 2 mm and for the angles at 20°.
From this a fitness for arbitrary individual, j, is calculated, using the following formula[8]:

$$fitness(j) = \sqrt{\left(\frac{PP_{x,demand} - PP_x}{W_x}\right)^2 + \left(\frac{PP_{z,demand} - PP_z}{W_z}\right)^2 + \left(\frac{\alpha_{demand} - \alpha}{W_\alpha}\right)^2 + \left(\frac{\beta_{demand} - \beta}{W_\beta}\right)^2} \tag{2.6}$$

2.6.2 Numerical approach: results and conclusion

When several values have been set for the use of the algorithm: distance parameters (d, l and ypp), the demanded position, angle ($\vec{PP}_{demand}, \alpha_{demand}$ and β_{demand}) and a number of generations an individual is received containing the best θ_1, θ_2, ϕ_1 and ϕ_2.

[5] The source, however, should be able to give a clear view on the details.
[6] The algorithm is provided in Matlab coding, which is also the program used during the bachelor's assignment for the numerical work done (version: R2012a).
[7] These values were approximated, looking at the mirrors' dimensions and an estimated setup where a 20°deflection would suffice.
[8] For the full Matlab script see appendix B.

When Jeroen Korterik was changing some of these values he found that when α was kept stationary at 10°and β was varied between 0 and 10°the angle of the mirror in the same plane as α only changes with 0.002°. This error is perhaps within acceptable parameters, therefore this might indicate that the coupling is pretty weak and hence the analytical model might be revised and simplified.

Nonetheless it seems a numerical approach is able to provide the system with a set of useable angles (individuals). However, this has not yet been done but should be easily solvable with a for-loop calculating all α and β of the scan region.

CHAPTER 3

GALVANOMETER-MIRRORS

3.1 Introduction

Before even starting this bachelor's assignment, Jeroen had already bought a galvanometer-mirror system. The systems are reasonably widely available as they are used in laser shows, hence a lot of amateur enthusiasts use them. Yet there is only very little documentation available about the GM-mirror systems[1]. In order to get the best possible resolution, all systems of the LSCM have to be as accurate as possible. Hence one part of the assignment was to characterize the GM systems.

3.2 GM settings

The GM systems included in substance two parts: two mounted mirrors with their galvanometers and a feedback system. The feedback system has some adjustable trimmer potentiometers, which change the system. Three settings were of importance: servo gain (SG), low frequency damping (LFD) and high frequency damping (HFD)[2]. This control system was put inside a box so it could be flexibly used, see figure 3.1.

So before the system could be used the SG, LFD and HFD had to be set in the best possible way where the mirrors would follow the signal as fast and precise as possible. As the settings were blindly adjustable, there was no readout, apart form the mirror's behaviour, there is no real way of knowing their actual value. However, it is still possible to tell their effect by looking at the behavior of the mirror. In the manual of the GM-system a reference to a testing pattern called ILDA is referred at, see appendix C. The most important features in this pattern are the middle circle and the square around the circle. By adjusting the three settings the shape and under- or overshoot can be adjusted for. However, this proved not to be ideal for laser sample scanning as the step-response proved not to be optimal. Therefore another protocol was used, invented by Jeroen. For one of the results see figure 3.2. Changing one of the settings, SG, LFD or HFD would change this figure as the system was or was not able to show the desired pattern. An ideal pattern would be where the horizontal lines would be perfectly cornered to the vertical lines, which should be straight, i.e. no under- or overshoot.

The calibration method was to use two different signals for the x or y GM. Depending on which GM was calibrated a square wave and a triangular wave were used. Both waves have the same frequency. The triangular wave can be compared to a time axis while the square wave shows the system's response. By adjusting the settings it was then possible to improve the visible laser light; to make the laser square as similar as possible to the electrical signal: a near perfect square wave. To increase the ease with which the system was visualized a small phase offset of the signals was used to move/change the laser pattern. When the corners where clear the frequencies were equalled again so the system could be optimized.

Furthermore, the box requires normal socket power input and a steering signal of max. $\pm$5V. Besides this, the box is linked with the galvanometers, providing feedback as well.

[1] The GM-system that was used for designing the microscope was a "High speed Galvo System, AXJ-V20 close-loop scanner".
[2] The way and theory about how these settings influence the system will be discussed in section 3.3.

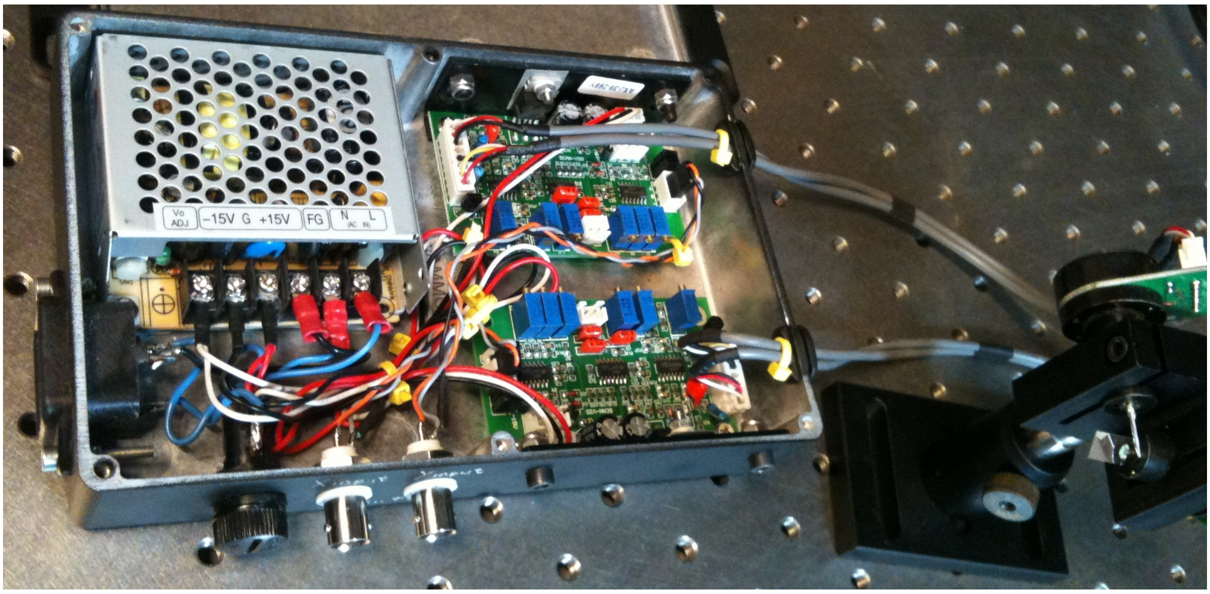

Figure 3.1: The control box for one GM-mirror system. The two circuit boards are for one of the mirrors, some of the blue rectangles are the trimming potentiometers, which change SG, LFD or HFD, amongst other settings. On the right side of the picture the mirror system is also visible.

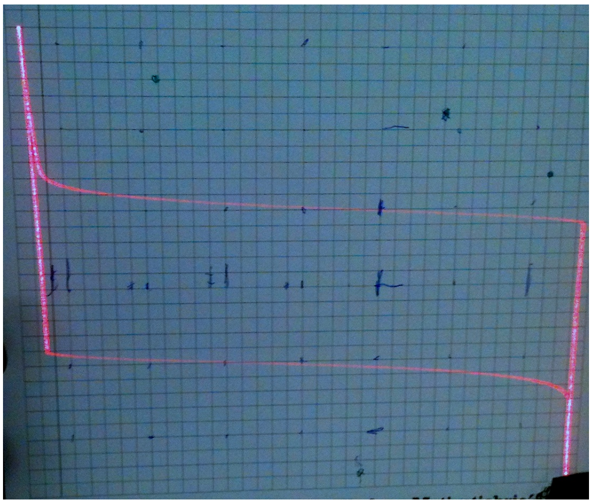

Figure 3.2: Step response laser lines of galvanometer 2 (GM2). The x-axis follows a square-wave of which the frequency was 50Hz. The y-axis follows a triangular wave with a frequency of 50Hz. X/Y deflections are 17.5°. Note that at the bottom-left corner of the laser still a slight amount of overshoot is visible.

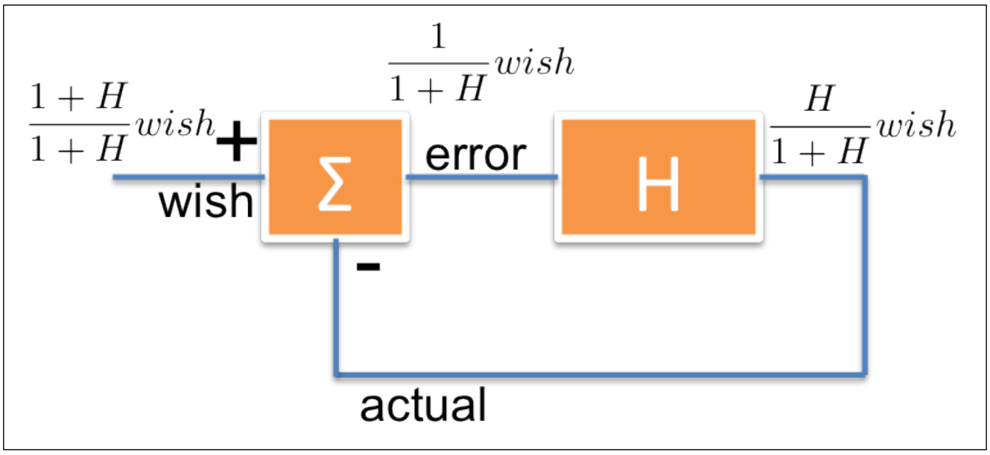

Figure 3.3: A feedback loop also viable for the GM systems. Note that the H-block includes the servo gain, galvanometer and a sensor (see fig. 3.4).

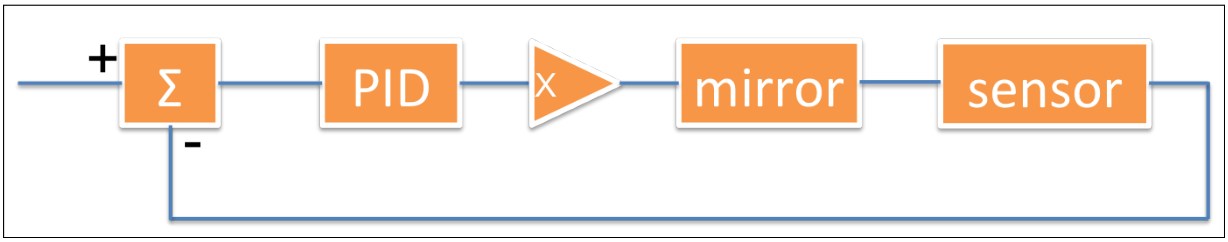

Figure 3.4: A feedback loop also viable for the GM systems, where the block "H" of figure 3.3 has been expanded into a PID block, multiplication, mirror actuator and sensor (left to right).

3.3 Theoretical model

The GM system can be modeled as a feedback loop, as seen in figure 3.3. Which could be expanded to figure 3.4.

If this block is modeled in a log-log plot the open loop amplitude feedback as function of frequency mainly of a -2 slope, corresponding with a -180°phase. This is because the mirror is basically a simple $F = m * a$ system, with a second derivative of angular position. However, if a close look is taken at the behaviour of the closed loop the following formulas come into play:

$$\frac{1}{1+H}wish \quad \text{(Error)} \tag{3.1}$$

$$\frac{H}{1+H}wish \quad \text{(Response)} \tag{3.2}$$

$$\frac{1+H}{1+H}wish \quad \text{(Wish)} \tag{3.3}$$

3.3.1 Accuracy

H represents the amplitude with which the controller will respond. At very high values of H the mirrors will respond very strongly so the wish is followed well. Therefore H should be as high as possible for the relevant frequencies.

3.3.2 Stability

The system is stable as long as the amplitude does not equal 1 with a -180°phase for any frequency. In that case the response will be divided by 0 and hence oscillations will occur, see figure 3.6.

Hence a stopped differentiator[3] is introduced. This will give the log-log plot a local +1 slope, resulting in a total -1 slope in amplitude locally. But it also changes the phase of the feedback (H). Therefore the response will not divide by 0 and hence no oscillations take place.

The SG, LFD and HFD influence the behaviour of this system. The SG increases the total amplitude; it remains a -2 slope but with an offset. The LFD and HFD represent the frequency upper limits of the stopped differentiator. Where they need to be set to envelop the oscillation region: an amplitude of 1. Furthermore, since it decreases the response amplitude it is preferable that as little as possible of the slope is -1, so LFD and HFD should be as close to each other as possible, while still preventing oscillations. In order to prevent oscillations a rule of thumb is to have at least 55°phase increase because of the stopped oscillator.

In figures 3.5 and 3.6 two simulated responses are shown. Figure 3.5 shows a well set system. The closed loop response of the top log-log plot shows little increase in amplitude, so no alarming oscillations. The middle figure shows the phase and the red line the stopped differentiator's phase. Its peak is at -135°at the frequency where the amplitude passes 1, hence it is exactly the 55°margin at the right frequency. The bottom plot shows the time trace of the response and wish. For comparison also a wrongly set system is depicted in figure 3.6. In the middle plot it is seen that the LFD and HFD have been wrongly set, so the peak only reaches -151°: a margin of only 29°. This is clearly not enough as a 2x magnitude oscillation occurs (top log-log plot).

3.4 Characterisation - results

The measurements were done by measuring the amplitudes of x and y at various frequencies at several set deflections. One example measurement can be seen in figure 3.7. The x- or y-span of the image was measured using a caliper. When the laser hit the caliper a reflection was shown on the table, therefore it was a reasonably solid way to measure this. The errors made were estimated to be ±1mm. The z-distance was measured to be 475mm ±1mm. The results are shown in double logarithmic plots in figures 3.8-3.11.

Looking at the plots it is clear that both systems were optimized at different moments[4] as they behave quite differently. Looking at figure 3.10 and 3.11 (GM system 2) it is shown that they behave quite nicely, without any oscillations. However, system 1 shows some oscillating behaviour, especially in the y-span.

3.5 Conclusion and discussion

The double logarithmic plots show some similarities with the closed loops of the top plots of figures 3.5, 3.6. Oscillations are present and after a certain frequency the amplitudes keep reducing. GM 2 seems to be overly damped as no oscillation effect is seen at any frequency[5]. Both show little oscillations but they do not seem to be too severe for the system. The simulated data does not fit the general negative slope of the obtained data. This might be because the simulated data did not take into account any frictions. Also, the GMs suffer slew rate limitations. The response is limited by a limited drive current which is just a preset maximum and therefore cannot be corrected for by the feedback loop. This might also introduce a dynamic non-linearity as this effect is varying at different frequencies.

[3] An electrical circuit resulting in a local derivative behavior.

[4] A person has to tell when the system is optimized well enough, this is very objective and may not be constant.

[5] Even a good damped system should show some oscillation effect as seen in the simulations, figure 3.5.

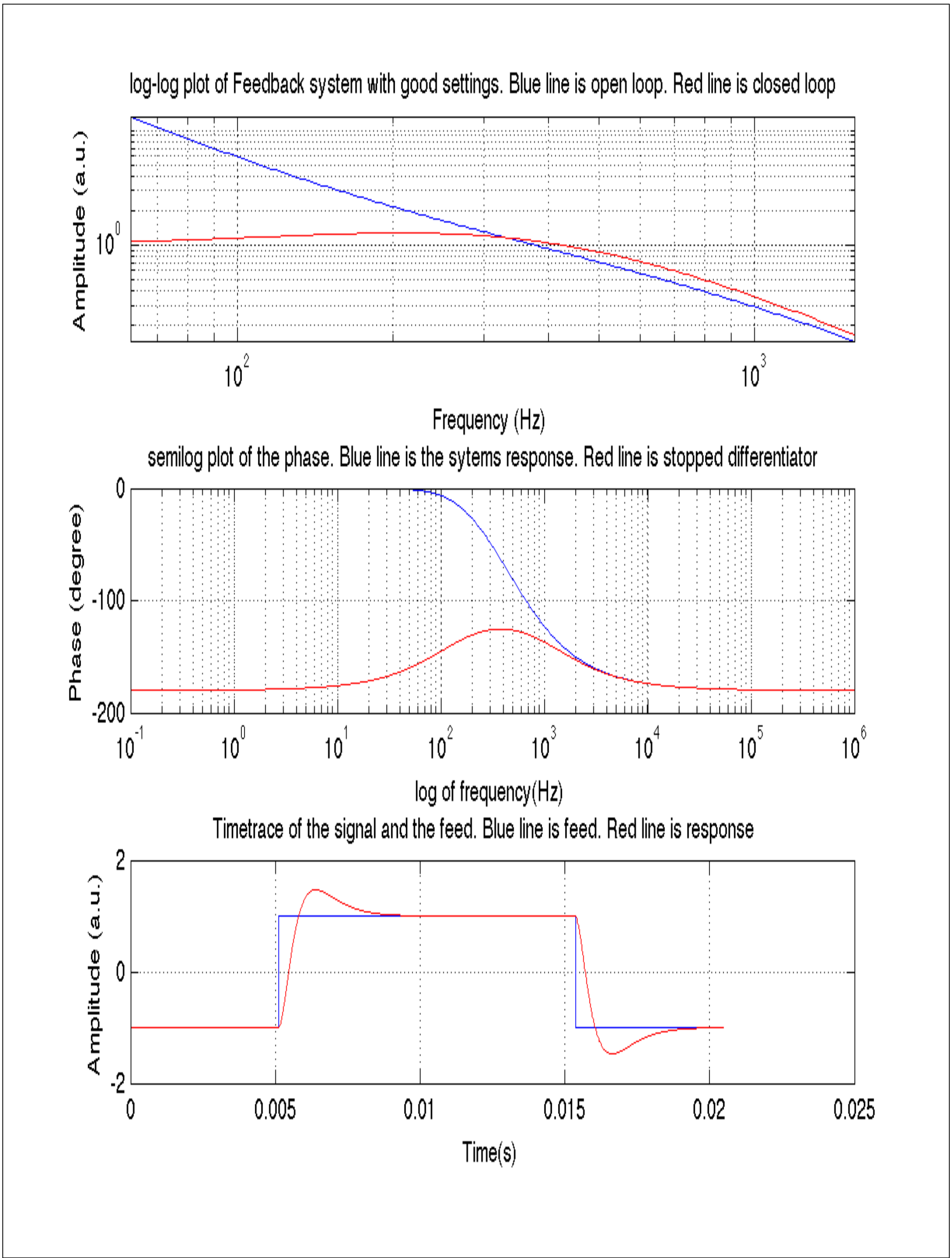

Figure 3.5: Simulink simulation of a well setup feedback loop.

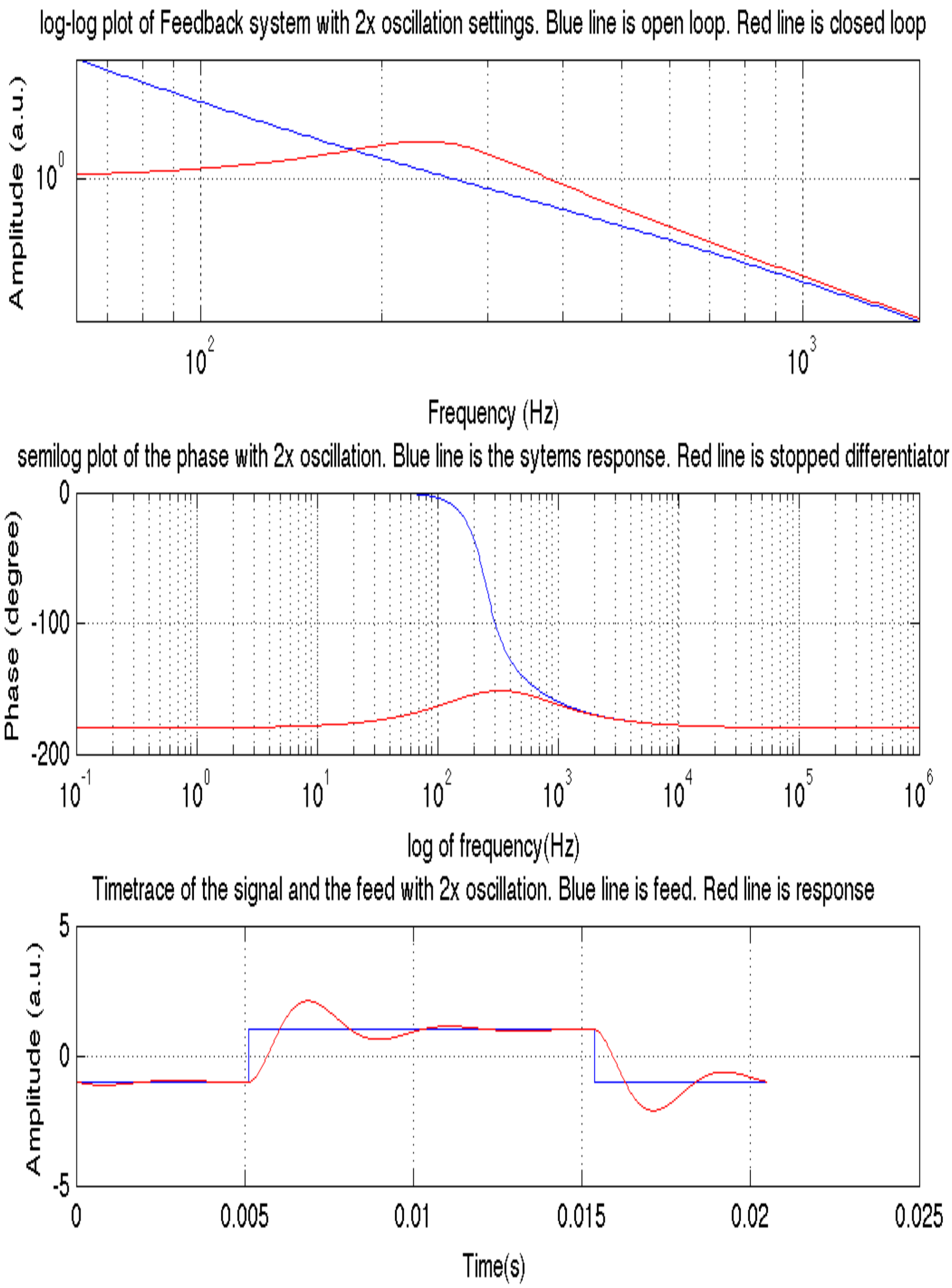

Figure 3.6: Simulink simulation of a system that has a 2x amplitude oscillation.

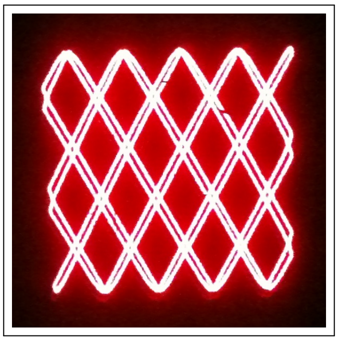

Figure 3.7: Example measurement of galvanometers. The total x and y spans were measured using a caliper.

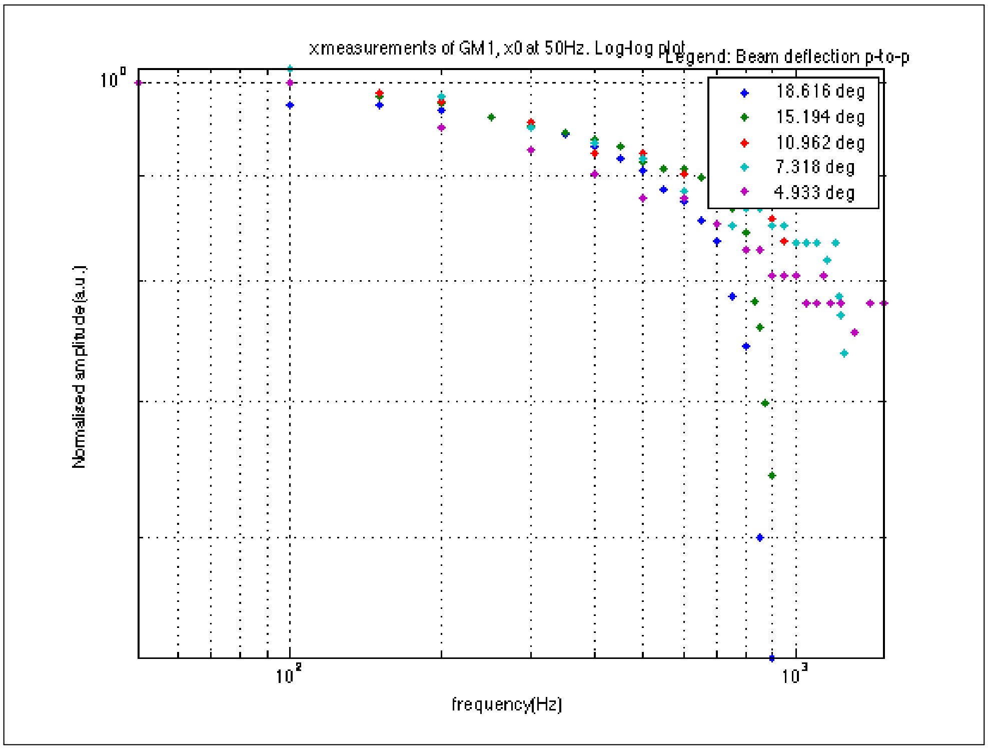

Figure 3.8: Log-log plot of measurement results of galvanometer 1, x span. System was optimized using the method described in section 3.2.

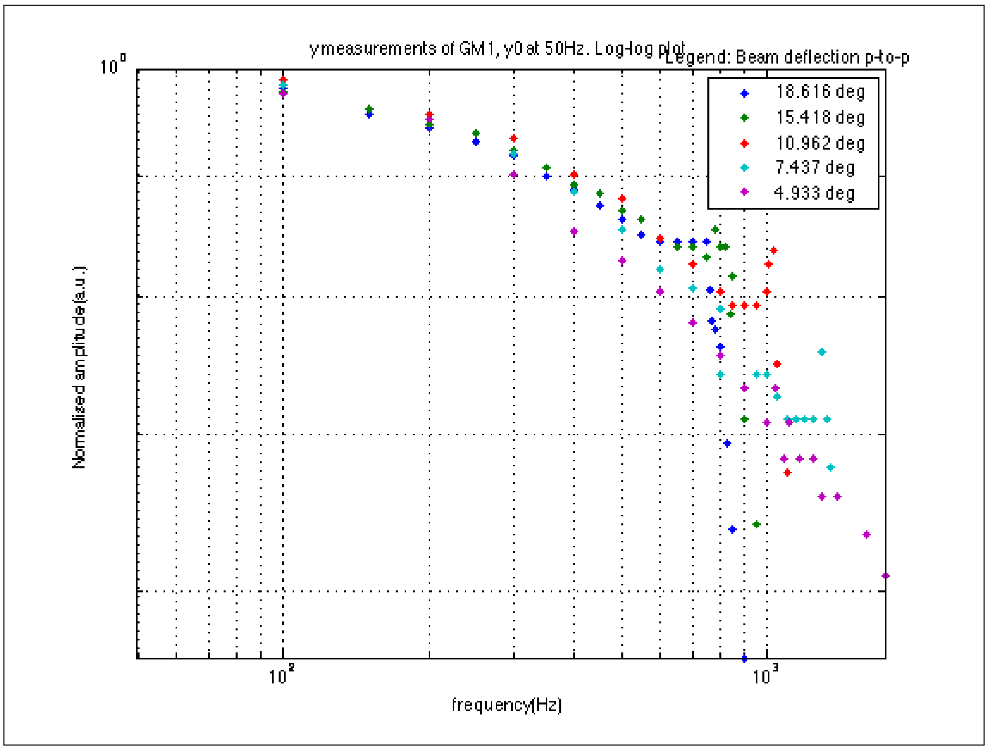

Figure 3.9: Log-log plot of measurement results of galvanometer 1, y span. System was optimized using the method described in section 3.2.

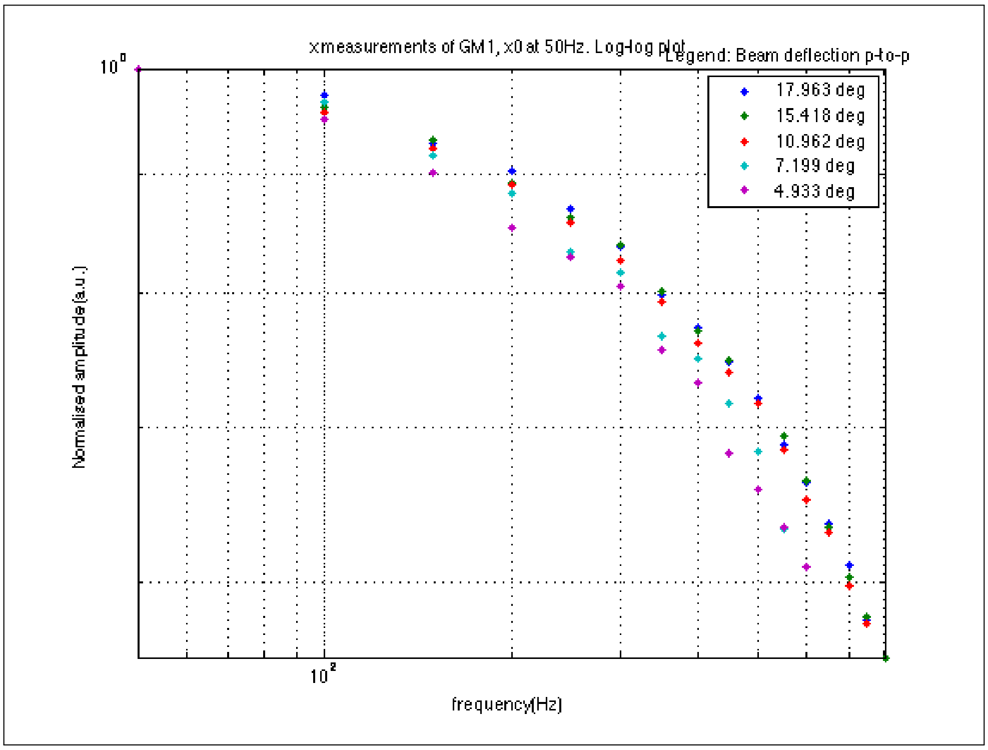

Figure 3.10: Log-log plot of measurement results of galvanometer 2, x span. System was optimized using the method described in section 3.2.

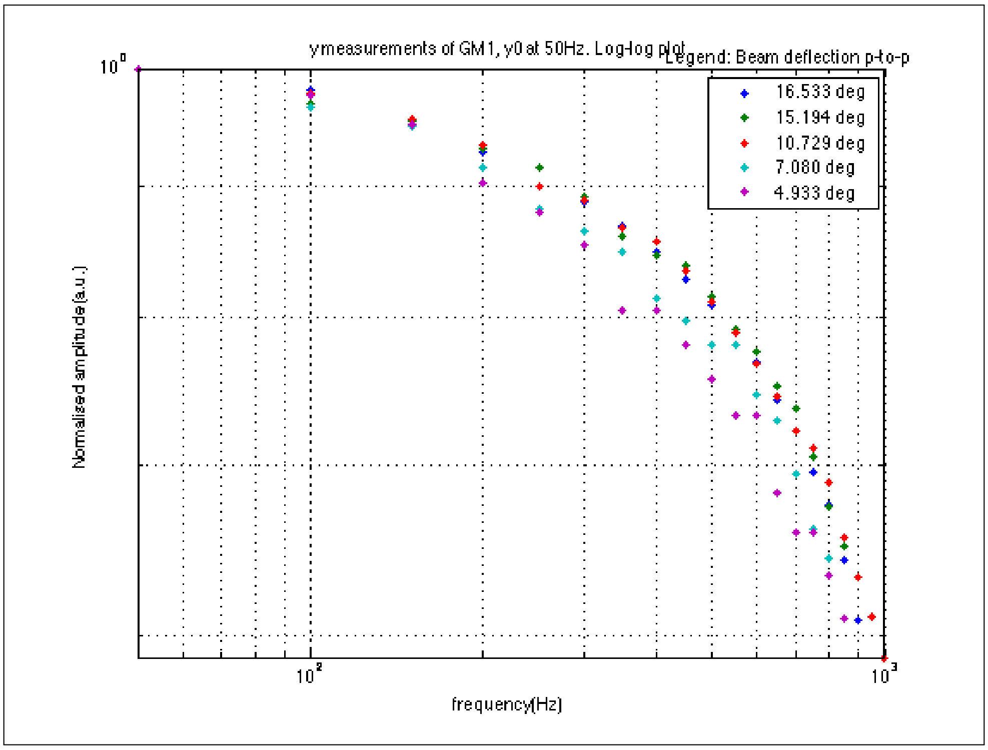

Figure 3.11: Log-log plot of measurement results of galvanometer 2, y span. System was optimized using the method described in section 3.2.

It should also be noted that the investigated frequency ranges of GM1 and GM2 differ. Both GMs behave non-linear at high frequencies, which is influenced by the GM's deflection. This behaviour includes different amplitudes when the frequency is either increased or decreased. This might indicate that it is a bi-stable system. Furthermore, at some times the GM jumped when passing a certain frequency[6]. When these effects occurred, the measurements had gone far enough as this non-linear behaviour is unwanted for a scan engine.

Furthermore, there might be some non-linearities in the feedback system. However, this might not be easy or possible to find. Looking at figure 3.4, there are several elements which bring about this error. If it is in the PID or mirror it will be detected by the sensor and it will be corrected for automatically. Therefore, this error will not be detectable. But if the error is present in the sensor this will be seen in the output, as it will not match the wish.

As the whole scan engine system has been evaluated; all aspects can be combined in a theoretical design. The location of PP and its desired angles can be calculated using the theoretical model. With the characterization done[7], it is now possible to determine what kind of voltage signal should be offered to the GM system to obtain the desired deflections. It is possible to linearly combine these aspects, as the deflection/PP calculation is independent of the characterisation.

[6] The GMs and their mounts warmed up as well.

[7] It would still be advisable to check the actual deflection at various voltages and frequencies, see chapter 5 point 1.

CHAPTER 4

OVERALL CONCLUSIONS

The scan engines currently used introduce some imperfections with them as only two mirrors are being used. Therefore, a new layout was made, introducing two extra mirrors. These extra mirrors not only counter the imperfections, but also give full 3D control of the stationary pivot point. The mathematical description that was made during this assignment was found, although it is quite extended and coupled. Several analytical approaches were tried in order to solve it but they proved not to lead to a solution. Therefore, another, numerical approach was tried using a covariant matrix adaptation (CMA) evolution strategy, where the same mathematical description was used. This CMA matrix proved to be useful to find a set of mirror deflections, thus proving its utility. The numerical approach also indicated that the analytical expression may be simplified. The system could possibly be modeled as two, 2-mirror systems; one for x or y each. This would prevent the coupling.

Furthermore, a set of galvanometer-mirrors was characterized. These systems were first put together in boxes for convenience, after which they were optimized to work in a scanning beam system. The deflections of the galvanometers were then measured as function of frequency at a set signal strength. Also, a theoretical model of the scan engine was suggested, based on the design and characterization results.

The changes in the scan engine can be used in a laser scanning confocal microscope. The microscope uses a lens system for which a true stationary point is required. Therefore, the designed system should improve aberrations in the scan engine compared to the current systems.

CHAPTER 5

RECOMMENDATIONS

Just starting with this bachelor's assignment the idea was to design and actually build a laser scanning confocal microscope. However, the design proved to be trickier than initially expected. Therefore, only parts of the design has been realised. That is to say: there is still quite some work to be done for the OS-group's very own built LSCM. Below, I will provide some aspects which I think should or could be done to finish or improve this project.

1. Characterising the electrical transfer to the galvanometers, $V_{in} \longrightarrow \theta/\phi$.
   Although some early measurements using a different tuning of the GMs[1] has shown that $angleV_{in}$ is in fact linear this is not certain with the other settings.

2. Design the general layout of the microscope.
   Some ideas:

   - Allow the sample to lay on a horizontal platform as this is easier with fluidic samples. However, some experiments rely on transmission through the sample. Therefore it might be required that other optics is possible behind the sample.

   - Introduce a way to allow depth scanning, e.g. through a sample stage.

3. Compare the aberrations of both lenses and off-axis parabolic reflectors (OAPs). Both systems have their aberration but it has not been investigated which distorts the image most. Literature states that OAPs bring several difficulties. Their alignment needs to be done very carefully [7]. However when use of a 4-mirror scan engine is made the alignment does not need be so precise. Another downside of using OAPs is that coma is introduced inherently, especially when a magnification is introduced [4]. Several simulations about the OAPs have been done by Jeffrey Reuling [6]. Jeffrey used the program Radiant Zemax[2] to model several layouts of OAPs.

4. Make sure to align the system well enough; do not rely too much on the alignment-repairing abilities of the scan engine. The mirrors only have a small area and hence cannot be offset too far as this can cause the beam to miss the mirrors.

5. Allow slight sample stage movement as not all areas of the sample are equally interesting to image.

6. Investigate if heat influences the GMs as they warm up at high frequencies.

7. Simplify the analytical model. Compare those results with the exact analytical model to find out its errors.

8. The XYXY layout has now been expressed mathematically, but other layouts are also possible, or preferable. One reason, however, is that this layout optimally uses the area of all mirrors. If for example a XXYY layout is used the X correction mirror needs to correct for a larger distance.

[1] This was done after the 'Frans Segerink laser show'.
[2] http://www.radiantzemax.com/

Bibliography

[1] Kenneth W. Dung, Exing Wang, Stephen W. Paddock, J. Hazen Eric, Peter J. DeVries, James B. Pawley, Jeffrey M. Larson, Stanley A. Schwartz, Matthew Parry-Hill, Thomas J. Fellers, and Michael W. Davidson. Nikon microscopyu — confocal microscopy, June 2013.

[2] E. T. Garbacik, R. P. Korai, E. H. Frater, J. P. Korterik, C. Otto, and H. L. Offerhaus. In planta imaging of ?9- tetrahydrocannabinolic acid in cannabis sativa l. with hyperspectral coherent anti-stokes raman scattering microscopy. *Journal of Biomedical Optics*, April 2013.

[3] Nikolaus Hansen and Andreas Ostermeier. Adapting arbitrary normal mutation distributions in evolution strategies: The covariance matrix adaptation. In *Evolutionary Computation, 1996., Proceedings of IEEE International Conference on*, pages 312–317. IEEE, 1996.

[4] Robert M Malone, Steven A Becker, Daniel H Dolan, Richard G Hacking, Randy J Hickman, Morris I Kaufman, Gerald D Stevens, and William D Turley. Design of a thermal imaging diagnostic using 90-degree, off-axis parabolic mirrors. In *Proc. SPIE*, volume 6288, page 62880Z, 2006.

[5] Stephen W Paddock. Principles and practices of laser scanning confocal microscopy. *Molecular biotechnology*, 16(2):127–149, 2000.

[6] Jeffrey Reuling. Simulation of 90-degree off-axis parabolic mirrors. *ELPNO*, June 2013.

[7] Galiya Sharafutdinova, John Holdsworth, and Dirk van Helden. Improved field scanner incorporating parabolic optics. part 1: simulation. *Applied optics*, 48(22):4389–4396, 2009.

[8] Peng Xi, Yujia Liu, and Qiushi Ren. Scanning and image reconstruction techniques in confocal laser scanning microscopy. *Laser Scanning, Theory and Applications, C.-C. Wang, ed.(Intech Open, 2009)*, pages 523–542, 2009.

ACKNOWLEDGMENTS

A lot of people have helped me during the course of my assignment at the Optical Sciences group and I would like to thank all of them.

I really liked working at the OS group. And although the most alluring aspect should be research this is not the key reason why I enjoyed my time here so much. The atmosphere and its members are really, really pleasant. And in the student room, although it has probably changed right now, was good as well. In there the topics were explained by peers, who helped me grasp their topics better. The research presented on every Tuesday is also really interesting, giving me a slight glimpse of all of OS' research.

My interest in optics really took off when I was lucky enough to attend Jennifer's lectures.

But no one can surpass Erik's enthusiasm. After the course Introduction to Optics of Jennifer I asked Jennifer whether I could visit once and see what the group was like and what kind of research they were doing. We made an appointment and a full OS-tour was organized, done by Erik. After this tour I was hooked on OS and I made the decision to do my bachelor's assignment here. During my first few weeks here I must have tested Erik's patience as I was a true newbie to optics. But he remained enthusiastic and helped me enormously, sending me on quests, giving me direction on what steps to take next.

And numerous thanks to Jeroen. When I had a question or difficulty with anything, I could come to him and he would help me. As he is of the technical staff, a lot of his guidance was with practical work, for example he taught me the basics of soldering used on the boxes, which I had never done before. But also with the experiments he would give me tips and get me going. Moreover, he taught me a lot of the basics of some electronics and feedback systems in multiple informative discussions.

Herman kept me on track. At the meeting with Jeroen and Erik he suggested several deadlines, which made me realize I had to step up my pace and work a little more towards results. Also Herman made the group lunches pleasant to attend; when he was present he always was the centre of some discussion about a random topic.

Also I would like to thank Mark for doing this. In my opinion I was a bit late with informing you and with involving you in this assignment but you assured me it was not too late: thanks.

Lastly I would like to thank my fellow board members of Astatine, my flat: Calslaan 18, DKV Euros and the band for the interest, support and understanding I was not always that actively involved. And thanks for making me wonder myself, what I actually was doing at OS at the start, as I actually was not really sure myself. Moreover I want to thank Frank Vermeulen and Remco Bastiaannet for critically reading my report and for giving me tips on it.

Appendices

Appendix A

Derivation of the Stationary point

For convenience the figures used for the derivation have been shown again.

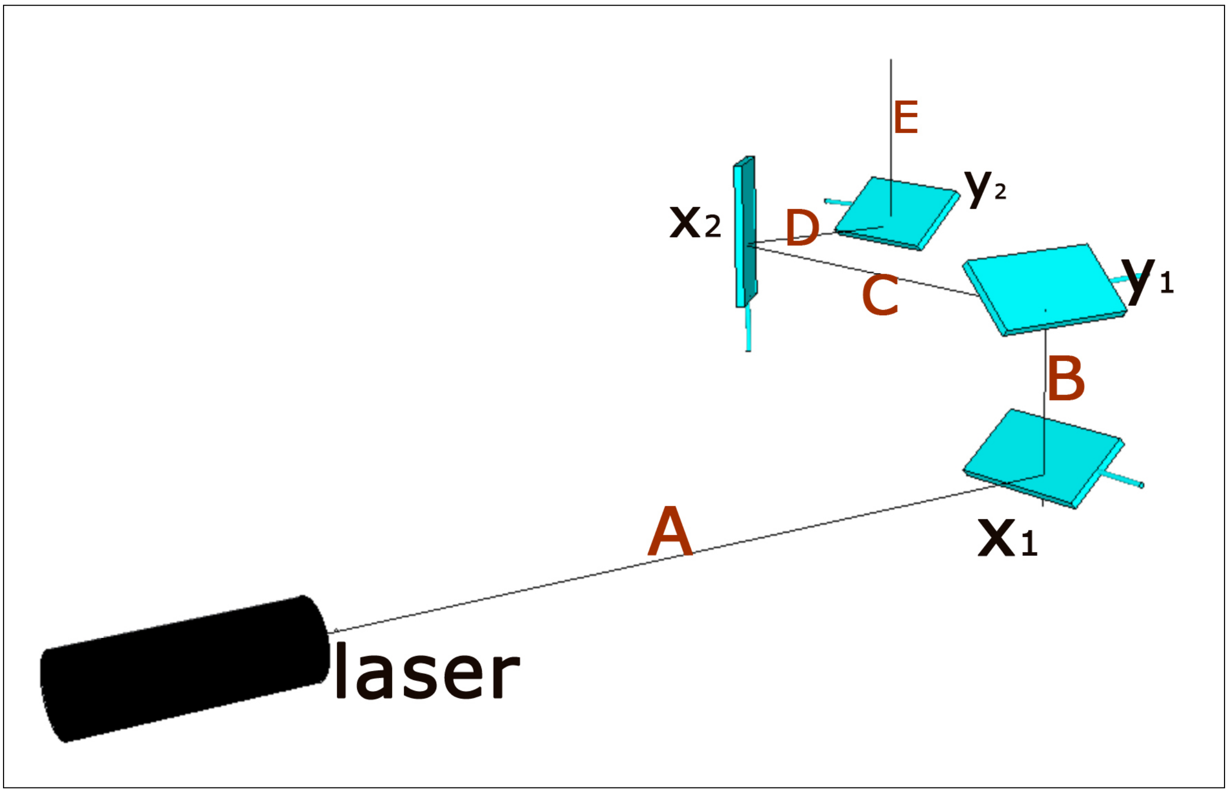

Figure A.1: Lay out of the scan engine and its mirrors: X1, Y1, X2 and Y2. In this setting the scan area would be in the z, x plane but this can of course easily be changed by adding another 45°mirror.

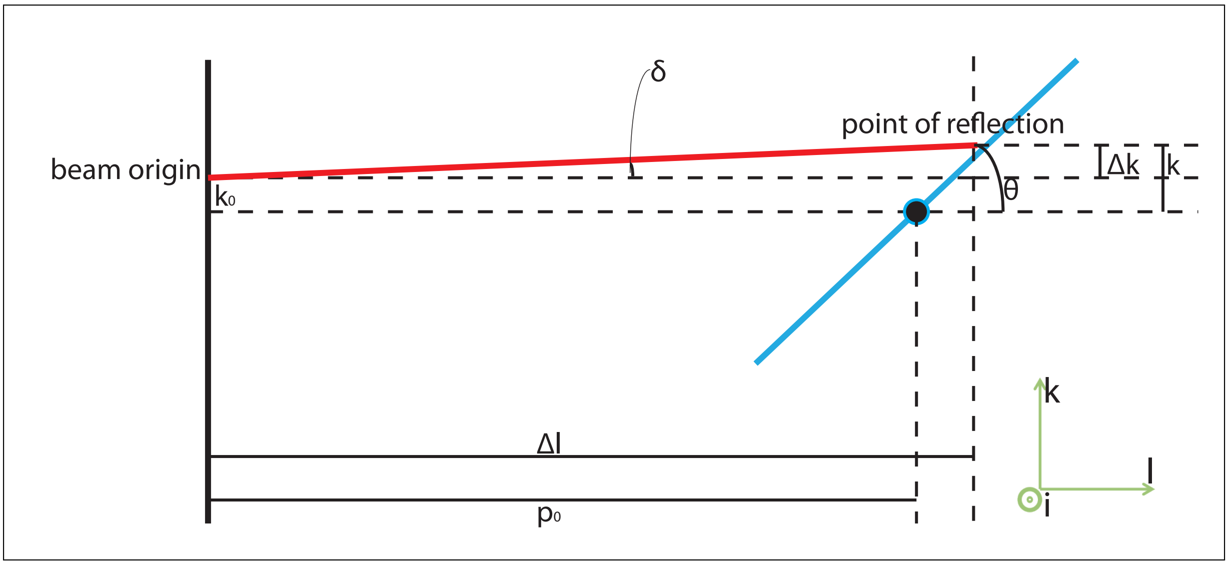

Figure A.2: The Cheatsheet, l and k view.

$$\Delta l = \frac{\Delta k}{\tan(\delta)} \tag{A.1}$$

$$k = (\Delta l - pp_0)\tan(\theta) \tag{A.2}$$

$$\Delta l = \frac{(\Delta l - p_0)\tan(\theta) - k + 0}{\tan(\delta)} \tag{A.3}$$

$$= \frac{\Delta l \tan(\theta) - p_0 \tan(\theta) - k_0}{\tan(\delta)} \tag{A.4}$$

$$\Delta l - \Delta(\frac{\tan(\theta)}{\tan(\delta)} = \frac{p_0 \tan(\theta) - k_0}{\tan(\delta)} \tag{A.5}$$

$$\Delta l \left(1 - \frac{tan(\theta)}{\tan(\delta)}\right) = \frac{p_0 \tan(\theta) - k_0}{\tan(\delta)} \tag{A.6}$$

$$\boxed{\Delta l = \frac{p_0 \tan(\theta) - k_0}{\tan(\delta) - \tan(\theta)}} \tag{A.7}$$

$$\Delta k = \Delta l \tan(\delta) \tag{A.8}$$

$$\boxed{\Delta k = \frac{p_0 \tan(\theta)\tan(\delta) - k_0 \tan(\delta)}{\tan(\delta) - \tan(\theta)}} \tag{A.9}$$

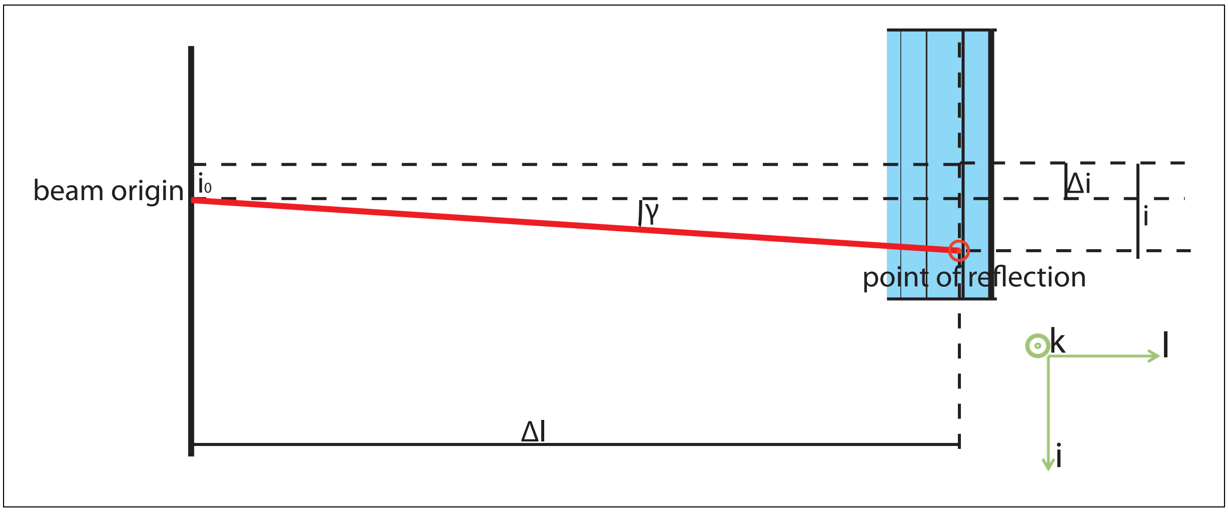

Figure A.3: The Cheatsheet, l and i view.

$$\Delta i = \Delta l \tan(\gamma) \tag{A.10}$$

$$\boxed{\Delta i = \frac{p_0 \tan(\theta)\tan(\gamma) - k_0 \tan(\gamma)}{\tan(\delta) - \tan(\theta)}} \tag{A.11}$$

Locations of deflection

It is possible to determine the location and the deflections of the ray using these equations and the fact that the mirrors are at positions:
-X1: (d, -l, -l)
-Y1: (d, 0, -l)
-X2: (0, 0, -l)
-Y2: (0, 0, 0)
with deflections of $\theta_1, \phi_1, \theta_2, \phi_2$ respectively.

Note that it is assumed that the laser is well aligned and therefore is axial with no offset with respect to the first mirror: X1. Furthermore the laser is at a distance L (in z direction) from the first mirror: X1[1]. Some extra dimensions:

- X mirror - Y mirror (one mirror set): l.
- Y mirror - X mirror (between the mirror sets: d.
- Last mirror to the pivot point: ypp.

Furthermore it is assumed all mirrors make right angles with each other and the mirror deflections are 45°in rest and $\theta_1, \theta_2, \phi_1$ and ϕ_2 are the extra angles added to this 45°. A: Laser - X1:

[1]The origin of the ray segment is lower case and the final location is capital, e.g. in the first ray segment the ray starts at a and then propagates to A, where it is reflected upon the mirror. This also means that point A will be point b, as the ray cannot make a sudden jump in location.

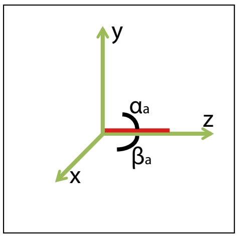

Where:
$\alpha_a = 0$
$\beta_a = 0$
a: (d, -l, -l-L)
$\boxed{A : (d, -l, -l)}$

B: X1 - Y1

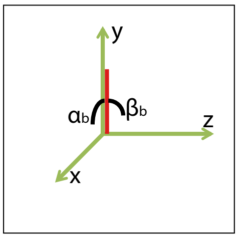

Where:
$\alpha_b = 0$
$\beta_b = 2\theta_1$
b=A: (d, -l, -l)

And substituting in eqs. A.7, A.9 and A.11:
$i = z, k = -x, l = y, \delta = -\alpha_b, \gamma = \beta_b, \theta = 0$[2],
$p_0 = l, k_0 = 0, i_0 = 0$

Gives:
$\Delta l = l$
$\Delta k = 0$
$\Delta i = -l \tan(\theta_1)$
$\Rightarrow \boxed{B : (d, 0, -l(1 + \tan(\theta_1))}$

C: Y1 - X2

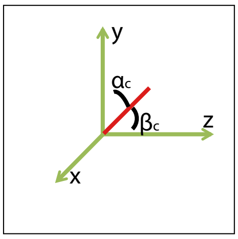

Where:
$\alpha_c = 2\theta_1$
$\beta_c = 2\phi_1$

[2]Note that this θ does not equal the mirror deflection, it is the θ from fig. A.2.

b=A: (d, -l, -l)

And substituting in eqs. A.7, A.9 and A.11:
$i = -y, k = z, l = -x, \delta = \beta_c \gamma = \alpha_c, \theta = 45° - \theta_2,$
$p_0 = d, k_0 = z_b - z_{Y1}, i_0 = y_b - y_{Y1}$

Gives: $\Rightarrow C =$

$$d - \frac{l\tan(\theta_1) + d\tan(-45+\theta_2)}{-\tan(2\theta_1) + \tan(-45+\theta_2)}, -\frac{l\tan(\theta_1)\tan(2\phi_1) + d\tan(-45+\theta_2)\tan(2\phi_1)}{-\tan(2\theta_1) + \tan(-45+\theta_2)}, -l(1+\tan(\theta_1)) + \frac{-l\tan(\theta_1)\tan(2\theta_1) - d\tan(-45+\theta_2)\tan(2\theta_1)}{-\tan(2\theta_1) + \tan(-45+\theta_2)}$$

<u>D: X2 - Y2</u>

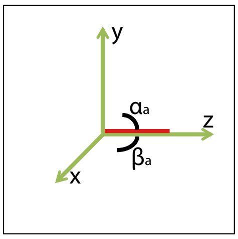

Where:
$\alpha_d = 2\phi_1$
$\beta_d = 2(\theta_1 + \theta_2)$
d=C

And substituting in eqs. A.7, A.9 and A.11:
$i = x, k = y, l = z, \delta = \alpha_d \gamma = \beta_d, \theta = 45° - \phi_2,$
$p_0 = l, k_0 = y_c - y_{Y2}, i_0 = x_c - x_{Y2}$

Gives: $\Rightarrow D =$

$$d - \frac{l\tan(\theta_1) + d\tan(-45+\theta_2)}{-\tan(2\theta_1) + \tan(-45+\theta_2)} + \frac{-\frac{\left(l\tan(\theta_1)\tan(2\phi_1) + d\tan(-45+\theta_2)\tan(2\phi_1)\right)\tan(2\theta_1+2\theta_2)}{-\tan(2\theta_1)+\tan(-45+\theta_2)} + \left(l(1+\tan(\theta_1)) - \frac{-l\tan(\theta_1)\tan(2\theta_1) - d\tan(-45+\theta_2)\tan(2\theta_1)}{-\tan(2\theta_1)+\tan(-45+\theta_2)}\right)\tan(-45+\phi_2)\tan(2\theta_1+2\theta_2)}{\tan(2\phi_1)+\tan(-45+\phi_2)},$$

$$-\frac{l\tan(\theta_1)\tan(2\phi_1) + d\tan(-45+\theta_2)\tan(2\phi_1)}{-\tan(2\theta_1) + \tan(-45+\theta_2)} + \frac{-\frac{\left(l\tan(\theta_1)\tan(2\phi_1) + d\tan(-45+\theta_2)\tan(2\phi_1)\right)\tan(2\phi_1)}{-\tan(2\theta_1)+\tan(-45+\theta_2)} + \left(l(1+\tan(\theta_1)) - \frac{-l\tan(\theta_1)\tan(2\theta_1) - d\tan(-45+\theta_2)\tan(2\theta_1)}{-\tan(2\theta_1)+\tan(-45+\theta_2)}\right)\tan(-45+\phi_2)\tan(2\phi_1)}{\tan(2\phi_1)+\tan(-45+\phi_2)}, -l(1+\tan(\theta_1))$$

$$+ \frac{-l\tan(\theta_1)\tan(2\theta_1) - d\tan(-45+\theta_2)\tan(2\theta_1)}{-\tan(2\theta_1) + \tan(-45+\theta_2)} + \frac{-\frac{l\tan(\theta_1)\tan(2\phi_1) + d\tan(-45+\theta_2)\tan(2\phi_1)}{-\tan(2\theta_1)+\tan(-45+\theta_2)} + \left(l(1+\tan(\theta_1)) - \frac{-l\tan(\theta_1)\tan(2\theta_1) - d\tan(-45+\theta_2)\tan(2\theta_1)}{-\tan(2\theta_1)+\tan(-45+\theta_2)}\right)\tan(-45+\phi_2)}{\tan(2\phi_1)+\tan(-45+\phi_2)}$$

For the last part, to the stationary pivot point, PP, Simple use of an offset line was used. So now Δk and Δi can easily be added to the coordinate of D. The offsets: k_0, i_o have no influence on Δs. However l_0 still has an influence on it: $p_0 = ypp - y_D - y_{Y2}$.

And using: $\boxed{\alpha_e = 2(\phi_1 + \phi_2)}$ and $\boxed{\beta_e = 2(\theta_1 + \theta_2)}$.

Gives: $\Rightarrow PP =$

$$2\,d-\frac{2\left(l\tan\left(\theta_1\right)+d\tan\left(-45+\theta_2\right)\right)}{-\tan\left(2\,\theta_1\right)+\tan\left(-45+\theta_2\right)}$$

$$+\frac{2\left(-\frac{\left(l\tan\left(\theta_1\right)\tan\left(2\,\phi_1\right)+d\tan\left(-45+\theta_2\right)\tan\left(2\,\phi_1\right)\right)\tan\left(2\,\theta_1+2\,\theta_2\right)}{-\tan\left(2\,\theta_1\right)+\tan\left(-45+\theta_2\right)}+\left(l\left(1+\tan\left(\theta_1\right)\right)-\frac{-l\tan\left(\theta_1\right)\tan\left(2\,\theta_1\right)-d\tan\left(-45+\theta_2\right)\tan\left(2\,\theta_1\right)}{-\tan\left(2\,\theta_1\right)+\tan\left(-45+\theta_2\right)}\right)\tan\left(-45+\phi_2\right)\tan\left(2\,\theta_1+2\,\theta_2\right)\right)}{\tan\left(2\,\phi_1\right)+\tan\left(-45+\phi_2\right)}$$

$$+\left(ypp+\frac{l\tan\left(\theta_1\right)\tan\left(2\,\phi_1\right)+d\tan\left(-45+\theta_2\right)\tan\left(2\,\phi_1\right)}{-\tan\left(2\,\theta_1\right)+\tan\left(-45+\theta_2\right)}\right.$$

$$\left.-\frac{-\frac{\left(l\tan\left(\theta_1\right)\tan\left(2\,\phi_1\right)+d\tan\left(-45+\theta_2\right)\tan\left(2\,\phi_1\right)\right)\tan\left(2\,\phi_1\right)}{-\tan\left(2\,\theta_1\right)+\tan\left(-45+\theta_2\right)}+\left(l\left(1+\tan\left(\theta_1\right)\right)-\frac{-l\tan\left(\theta_1\right)\tan\left(2\,\theta_1\right)-d\tan\left(-45+\theta_2\right)\tan\left(2\,\theta_1\right)}{-\tan\left(2\,\theta_1\right)+\tan\left(-45+\theta_2\right)}\right)\tan\left(-45+\phi_2\right)\tan\left(2\,\phi_1\right)}{\tan\left(2\,\phi_1\right)+\tan\left(-45+\phi_2\right)}\right)\tan\left(2\,\theta_1+2\,\theta_2\right),$$

$$ypp,\ -2\,l\left(1+\tan\left(\theta_1\right)\right)+\frac{2\left(-l\tan\left(\theta_1\right)\tan\left(2\,\theta_1\right)-d\tan\left(-45+\theta_2\right)\tan\left(2\,\theta_1\right)\right)}{-\tan\left(2\,\theta_1\right)+\tan\left(-45+\theta_2\right)}$$

$$+\frac{2\left(-\frac{l\tan\left(\theta_1\right)\tan\left(2\,\phi_1\right)+d\tan\left(-45+\theta_2\right)\tan\left(2\,\phi_1\right)}{-\tan\left(2\,\theta_1\right)+\tan\left(-45+\theta_2\right)}+\left(l\left(1+\tan\left(\theta_1\right)\right)-\frac{-l\tan\left(\theta_1\right)\tan\left(2\,\theta_1\right)-d\tan\left(-45+\theta_2\right)\tan\left(2\,\theta_1\right)}{-\tan\left(2\,\theta_1\right)+\tan\left(-45+\theta_2\right)}\right)\tan\left(-45+\phi_2\right)\right)}{\tan\left(2\,\phi_1\right)+\tan\left(-45+\phi_2\right)}+\left(ypp\right.$$

$$+\frac{l\tan\left(\theta_1\right)\tan\left(2\,\phi_1\right)+d\tan\left(-45+\theta_2\right)\tan\left(2\,\phi_1\right)}{-\tan\left(2\,\theta_1\right)+\tan\left(-45+\theta_2\right)}$$

$$\left.-\frac{-\frac{\left(l\tan\left(\theta_1\right)\tan\left(2\,\phi_1\right)+d\tan\left(-45+\theta_2\right)\tan\left(2\,\phi_1\right)\right)\tan\left(2\,\phi_1\right)}{-\tan\left(2\,\theta_1\right)+\tan\left(-45+\theta_2\right)}+\left(l\left(1+\tan\left(\theta_1\right)\right)-\frac{-l\tan\left(\theta_1\right)\tan\left(2\,\theta_1\right)-d\tan\left(-45+\theta_2\right)\tan\left(2\,\theta_1\right)}{-\tan\left(2\,\theta_1\right)+\tan\left(-45+\theta_2\right)}\right)\tan\left(-45+\phi_2\right)\tan\left(2\,\phi_1\right)}{\tan\left(2\,\phi_1\right)+\tan\left(-45+\phi_2\right)}\right)\tan\left(2\,\phi_1+2\,\phi_2\right)$$

Appendix B

Matlab CMA m-file

The Matlab file:[1]

```

%CMA for the Galvomirrorsystem.
%Inputs are 4 angles:theta1, theta2, phi1, phi2.
%Outputs are the position: PP and angles alpha and beta.



clear all; close all; clc
addpath C:\CMA
%addpath C:\Documents and Settings\jeroen\Desktop\David Dropbox\Dropbox\DvD BSc ...
    assignment\3.Simulation\Scan Engine GMs\Numerical\c_cma
genes = Initialization('myoptionsdavid.m');

%%%%% Set these as you want PP and angles %%%%%
PPxos = 0   /1000; % Off-set of PivotPoint - x [mm]
PPzos = 0   /1000; % Off-set of PivotPoint - z [mm]
aos = 10 *2*pi/360; % Wanted angle alpha - off-set [deg]
bos = -1 *2*pi/360; % Wanted angle beta - off-set [deg]


NumberOfGenerations = 400;

%%%%% Change these to specify the correctness of PP and angles %%%%%
xnorm = 2   /1000; % Normalisation/weighing for fitness [mm]
znorm = 2   /1000; % [mm]
anorm = 20   *2*pi/360; % Angle alpha normalisation [deg]
bnorm = 20   *2*pi/360; % Angle beta [deg]

%%%%% Change these to indicate the range at which the mirrors scan %%%%%
t1sc = 20*2*pi/360; % Scaling of the angles, theta1, theta2, phi1 & phi2 resp.
t2sc = 40*2*pi/360; % All these should be changed according to their characterisation.
p1sc = 20*2*pi/360;
p2sc = 40*2*pi/360;
t1of = -0.5; % offsets to center mirror angle around 0 deg
t2of = -0.5;
p1of = -0.5;
p2of = -0.5;
bestFitness=0;
i = 1;
clip = 0;
while (bestFitness < 1E8 & i < 1000)
%for i=1:NumberOfGenerations
    for j=1:size(genes,2)
      % Symbol conversions (Maple-->Matlab):
      % d = d
      % l = l
      % ypp = ypp
      % t1 = theta_1
      % t2 = theta_2
      % p1 = phi_1
      % p2 = phi_2
```

[1] In the Matlab text a reference is made to a file named: 'myoptionsdavid.m'. This file contains the number of individuals and number of individuals that will pass onto the next generation.

```
        d = 0.15; l = 0.01; ypp = 0.005; % Respectively GM1/2 distance, X-Y mirror distance...
            , Last mirror - PP distance.
        t1 = (genes(1,j)+t1of) * t1sc; % Apply scalings to be used in calculation of PPx or...
             PPz
        t2 = (genes(2,j)+t2of) * t2sc;
        p1 = (genes(3,j)+p1of) * p1sc;
        p2 = (genes(4,j)+p2of) * p2sc;

        % Calculation of outputs.
        PPx = (2 * d) - 0.2e1 * (l * tan(t1) + d * tan((-45 + t2))) / (-tan(0.2e1 * t1) + ...
            tan((-45 + t2))) + 0.2e1 * (-(l * tan(t1) * tan((2 * p1)) + d * tan((-45 + t2))...
             * tan((2 * p1))) * tan(0.2e1 * t1 + (2 * t2)) / (-tan(0.2e1 * t1) + tan((-45 +...
             t2))) + (l * (0.1e1 + tan(t1)) - (-l * tan(t1) * tan(0.2e1 * t1) - d * tan...
            ((-45 + t2)) * tan(0.2e1 * t1)) / (-tan(0.2e1 * t1) + tan((-45 + t2)))) * tan...
            ((-45 + p2)) * tan(0.2e1 * t1 + (2 * t2))) / (tan((2 * p1)) + tan((-45 + p2))) ...
            + (ypp + (l * tan(t1) * tan((2 * p1)) + d * tan((-45 + t2)) * tan((2 * p1))) / ...
            (-tan(0.2e1 * t1) + tan((-45 + t2))) - (-(l * tan(t1) * tan((2 * p1)) + d * tan...
            ((-45 + t2)) * tan((2 * p1))) * tan((2 * p1)) / (-tan(0.2e1 * t1) + tan((-45 + ...
            t2))) + (l * (0.1e1 + tan(t1)) - (-l * tan(t1) * tan(0.2e1 * t1) - d * tan((-45...
             + t2)) * tan(0.2e1 * t1)) / (-tan(0.2e1 * t1) + tan((-45 + t2)))) * tan((-45 +...
             p2)) * tan((2 * p1))) / (tan((2 * p1)) + tan((-45 + p2)))) * tan(0.2e1 * t1 + ...
            (2 * t2));
        PPy = ypp; % Not a relevant output, but for completeness it is here.
        PPz = -0.2e1 * l * (0.1e1 + tan(t1)) + 0.2e1 * (-l * tan(t1) * tan(0.2e1 * t1) - d ...
            * tan((-45 + t2)) * tan(0.2e1 * t1)) / (-tan(0.2e1 * t1) + tan((-45 + t2))) + 0...
            .2e1 * (-(l * tan(t1) * tan((2 * p1)) + d * tan((-45 + t2)) * tan((2 * p1))) / ...
            (-tan(0.2e1 * t1) + tan((-45 + t2))) + (l * (0.1e1 + tan(t1)) - (-l * tan(t1) *...
             tan(0.2e1 * t1) - d * tan((-45 + t2)) * tan(0.2e1 * t1)) / (-tan(0.2e1 * t1) +...
             tan((-45 + t2)))) * tan((-45 + p2))) / (tan((2 * p1)) + tan((-45 + p2))) + (...
            ypp + (l * tan(t1) * tan((2 * p1)) + d * tan((-45 + t2)) * tan((2 * p1))) / (-...
            tan(0.2e1 * t1) + tan((-45 + t2))) - (-(l * tan(t1) * tan((2 * p1)) + d * tan...
            ((-45 + t2)) * tan((2 * p1))) * tan((2 * p1)) / (-tan(0.2e1 * t1) + tan((-45 + ...
            t2))) + (l * (0.1e1 + tan(t1)) - (-l * tan(t1) * tan(0.2e1 * t1) - d * tan((-45...
             + t2)) * tan(0.2e1 * t1)) / (-tan(0.2e1 * t1) + tan((-45 + t2)))) * tan((-45 +...
             p2)) * tan((2 * p1))) / (tan((2 * p1)) + tan((-45 + p2)))) * tan((2 * p1 + 2 *...
             p2));
        alpha = 2*(p1 + p2);
        beta = 2*(t1 + t2);

        %Store the avarage values of the last generation to use these values.
        PPXarr(j) = PPx;
        PPZarr(j) = PPz;
        Alphaarr(j) = alpha;
        Betaarr(j) = beta;

        % RMS of all 4 outputs is the fitness number, each normalised by some
        % appropriate factor.
        fitnesses(j) = sqrt(((PPxos-PPx)/xnorm)^2 +((PPzos-PPz)/znorm)^2 +((aos-alpha)/...
            anorm)^2 +((bos-beta)/bnorm)^2);
        fitnesses(j) = 1/fitnesses(j);
        end
      genes = NextGeneration(fitnesses);
        for j=1:size(genes,2)
            for g=1:4
                %genes(g,j)
                if genes(g,j)>0.999 || genes(g,j)<0.001
                    genes = Initialization('myoptionsdavid.m');
                    clip = clip + 1
                    i
                end
            end
        end
        [maxColVal, maxColIdx] = max(fitnesses);
        bestFitness = maxColVal;
        i = i + 1;

    end
    %PPmm = [mean(PPXavg) PPy mean(PPZavg)].*1000 % In milimeters
```

```
%alphadeg = mean(Alphaavg)/pi/2*360 % In degrees
%betadeg = mean(Betaavg)/pi/2*360 % In degrees
%[maxColVal, maxColIdx] = max(fitnesses);
bestX=PPXarr(maxColIdx)*1000
bestZ=PPZarr(maxColIdx)*1000
bestAlpha=Alphaarr(maxColIdx)*360/(2*pi)
bestBeta=Betaarr(maxColIdx)*360/(2*pi)
i
j=maxColIdx;
%retreive mirror angles of best individual
t1 = (genes(1,j)+t1of) * t1sc; % Apply scalings to be used in calculation of PPx or PPz
t2 = (genes(2,j)+t2of) * t2sc;
p1 = (genes(3,j)+p1of) * p1sc;
p2 = (genes(4,j)+p2of) * p2sc;
t1deg = t1 * 360 / (2*pi)
t2deg = t2 * 360 / (2*pi)
p1deg = p1 * 360 / (2*pi)
p2deg = p2 * 360 / (2*pi)
%bestFitness
```

APPENDIX C

ILDA PATTERN

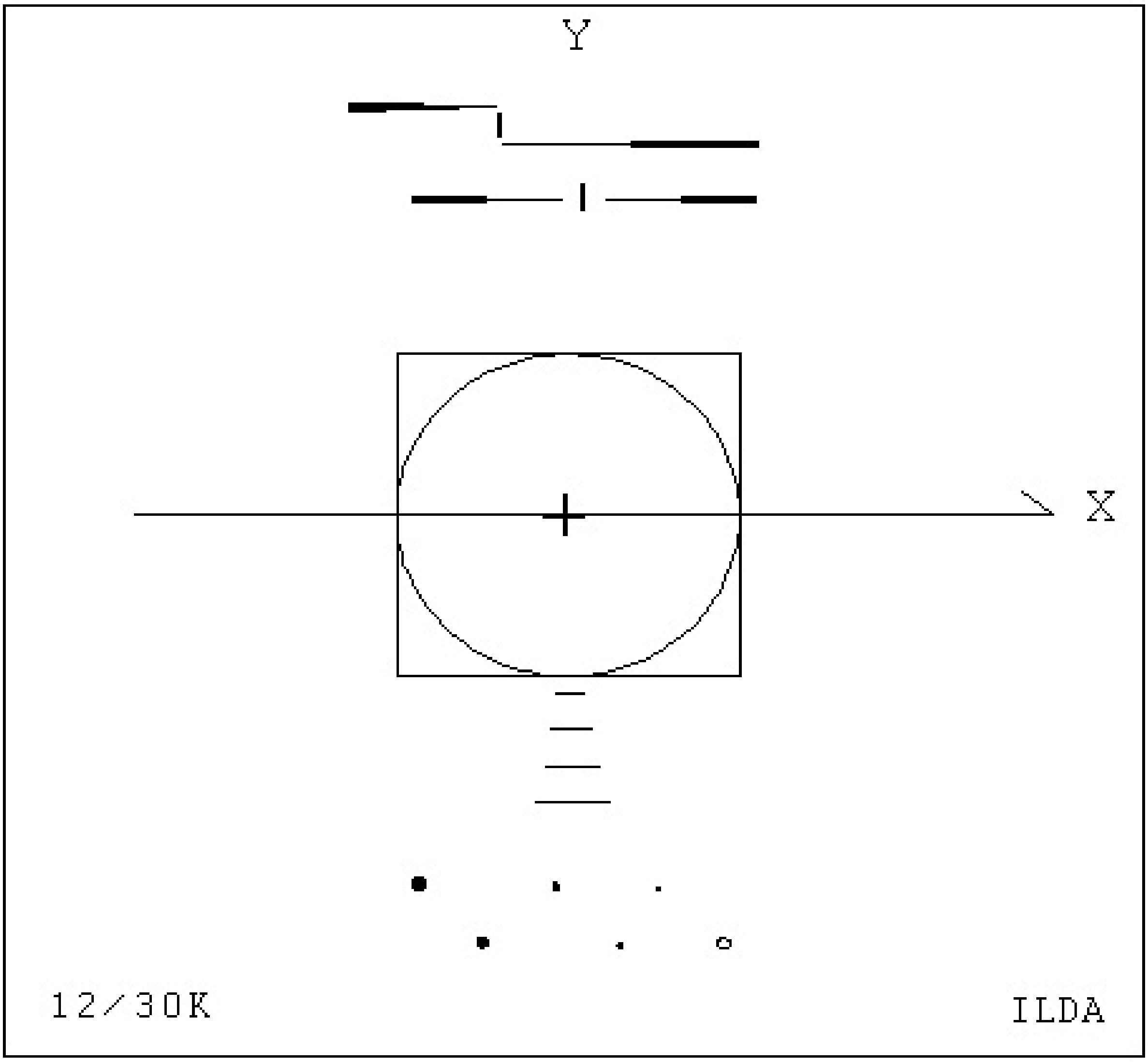

Figure C.1: ILDA test pattern. Source: http://www.laserfx.com/Backstage.LaserFX.com/Systems/Scanning3.html.

The actual optimization and use of the ILDA pattern is described on its site: http://www.laserfx.com/Backstage.LaserFX.com/Systems/Scanning3.html.